NOVEL MEMBRANE AND DEVICE FOR DIRECT CONTACT MEMBRANE DISTILLATION BASED DESALINATION PROCESS

New Jersey Institute of Technology
Newark NJ

Agreement Assistance No. 99-FC-810-180

Desalination and Water Purification Research and Development
Program Report No. 87

March 2001

U.S. DEPARTMENT OF THE INTERIOR
Bureau of Reclamation
Technical Service Center
Water Treatment Engineering and Research Group

REPORT DOCUMENTATION PAGE

Form Approved
OMB No. 0704-0188

1. AGENCY USE ONLY *(Leave Blank)*	2. REPORT DATE 3/30/01	3. REPORT TYPE AND DATES COVERED
		Final

4. TITLE AND SUBTITLE

NOVEL MEMBRANE AND DEVICE FOR
DIRECT CONTACT MEMBRANE DISTILLATION-BASED
DESALINATION PROCESS

5. FUNDING NUMBERS
99-FC-81--0180

6. AUTHOR(S) K.K. Sirkar and Yingjie Qin

7. PERFORMING ORGANIZATION NAME(S) AND ADDRESS(ES)
New Jersey Institute of Technology
Center for Membrane Technologies
Room 362 Tiernan Hall
Dr. Martin Luther King Jr. Blvd
Newark, NJ 07102

8. PERFORMING ORGANIZATION REPORT NUMBER

9. SPONSORING/MONITORING AGENCY NAME(S) AND ADDRESS(ES)
Bureau of Reclamation
Denver Federal Center
PO Box 25007
Denver CO 80225-0007

10. SPONSORING/MONITORING AGENCY REPORT NUMBER

11. SUPPLEMENTARY NOTES

12a. DISTRIBUTION/AVAILABILITY STATEMENT

Available from the National Technical Information Service, Operations Division,
5285 Port Royal Road, Springfield, Virginia 22161

12b. DISTRIBUTION CODE

13. ABSTRACT *(Maximum 200 words)* ***Direct contact membrane distillation (DCMD) and vacuum membrane distillation (VMD) of brine for desalination suffer from long-term flux decay due to membrane pore wetting and low water flux due to poor transport coefficients in the hot brine. Preliminary studies were carried out to address these problems. To prevent pore wetting, modules having an ultrathin microporous silicone coating on the surfaces of hydrophobic porous polypropylene hollow fibers were employed. Using a parallel flow Module 4 and high water velocity yielded a water flux of 15 kg/m^2-h at 91°C in VMD. There was no pore wetting even after a cumulative experimental duration of 1000 hours. In DCMD and VMD, a radial cross flow module and uncoated fibers yielded low water vapor fluxes. A large rectangular module having fibers with a nonporous coating also yielded low water vapor flux in DCMD. Conductive heat loss was substantial in the fine fibers; the cross flow velocity was very small in the large module where the hydrophobic fluoropolymer coating hindered water permeation much more than that in Module 4. Large fiber diameter and wall thickness, silicone coating and higher cross flow velocity are expected to substantially enhance the water vapor flux.***

14. SUBJECT TERMS--

15. NUMBER OF PAGES

16. PRICE CODE

17. SECURITY CLASSIFICATION OF REPORT	18. SECURITY CLASSIFICATION OF THIS PAGE	19. SECURITY CLASSIFICATION OF ABSTRACT	20. LIMITATION OF ABSTRACT
UL	UL	UL	UL

NOVEL MEMBRANE AND DEVICE FOR DIRECT CONTACT MEMBRANE DISTILLATION BASED DESALINATION PROCESS

Dr. Kamalesh K. Sirkar
Dr. Yingie Qin
New Jersey Institute of Technology
Newark NJ

Agreement Assistance No. 99-FC-810-180

Desalination and Water Purification Research and Development
Program Report No. 87

March 2001

U.S. DEPARTMENT OF THE INTERIOR
Bureau of Reclamation
Technical Service Center
Water Treatment Engineering and Research Group

Mission Statements

U.S. Department of the Interior

The mission of the Department of the Interior is to protect and provide access to our Nation's natural and cultural heritage and honor our trust responsibilities to tribes.

Bureau of Reclamation

The mission of the Bureau of Reclamation is to manage, develop, and protect water and related resources in an environmentally and economically sound manner in the interest of the American public.

Disclaimer

Information contained in this report regarding commercial products or firms was supplied by those firms. It may not be used for advertising or promotional purposes and is not to be construed as an endorsement of any product or firm by the Bureau of Reclamation**.**

The information contained in this report was developed for the Bureau of Reclamation; no warranty as to the accuracy, usefulness, or completeness is expressed or implied.

ACKNOWLEDGMENTS

The research conducted under this contract was sponsored by Desalination Research and Development Program, Bureau of Reclamation, Denver, Colorado. The investigators acknowledge the availability of the larger developmental Module 5 from Applied Membrane Technology, Minnetonka, MN, at a cost far below the actual cost. Jignesh Sheth helped Dr. Yingjie Qin substantially during the experiments conducted between January and August 2000. Dr. Sudipto Majumdar helped in developing the entrance sections for the larger Module 5.

Table of Contents

List of Tables

page

List of Figures

page

Glossary

cm	centimeter
C	salt concentration
DCMD	direct contact membrane distillation
F	water permeation flux, kg/m^2h
Hg	mercury
hr	hour
I.D.	internal diameter
kg	kilogram
m	meter
MD	membrane distillation
O.D.	outside diameter
PDD-TFE	perfluoro dimethyl-dioxole-tetrafluoroethylene
P_{lumen}	pressure in lumen
P_{perm}	pressure in permeate
P_{shell}	pressure in shell
RO	reverse osmosis
T	temperature, °C
$T_{cool\text{-}in}$	temperature of cold distillate at module inlet, °C
$T_{cool\text{-}out}$	temperature of cold distillate at module exit, °C
$T_{hot\text{-}in}$	temperature of hot brine at module inlet, °C
$T_{hot\text{-}out}$	temperature of hot brine at module exit, °C
u	velocity in fiber lumen, cm/s
VMD	vacuum membrane distillation
V_{cold}, V_{feed}	volumetric flow rate of cold distillate and hot brine feed, respectively, ml/min
τ	residence time, s

1. Executive Summary

Although research and development studies to improve commercialized reverse osmosis and thermally-driven desalination processes are continuing, there exists a need to develop and evaluate alternate desalination technologies, e.g., membrane distillation (MD) which utilizes waste heat. The particular technique of direct contact membrane distillation (DCMD) wherein the hot brine flows on one side of a gas-filled porous hydrophobic hollow fiber membrane and the cold distillate flows on the other side of the membrane is of interest. The primary deficiencies of this technique are flux reduction due to long-term pore wetting and reduced brine-side heat and mass transfer coefficients.

To overcome these, this research has made a preliminary investigation of the MD process where two changes were introduced: (1) The membrane has a thin water-vapor permeable hydrophobic nonporous/microporous coating on the brine side to prevent pore wetting; (2) to increase the brine-side heat transfer coefficient, the brine feed has cross flow vis-à-vis the hollow fiber membranes. It is known that the vacuum membrane distillation (VMD) technique, wherein there exists vacuum instead of cold distillate flow on one side of the membrane, the other side having hot brine flow, can illuminate many features of the brine side of a DCMD process. Therefore extensive data were obtained by the VMD process.

Porous hydrophobic hollow fiber membranes employed were of polypropylene. These fibers were with or without a nonporous/microporous coating of silicone polymer or a fluoropolymer. Module designs employed parallel flow, radial cross flow and rectangular cross flow. The number of fibers in a module was varied between 78 to 6000. The hot water/brine feed temperature ranged between 40 and 91 ^{o}C in VMD and between 38 ^{o}C and 70 ^{o}C in DCMD. At high feed velocities through the fiber lumen, a water permeation flux as high as 15 kg/m^{2}h was achieved in VMD at 91 ^{o}C through a small parallel flow module (Module 4) having an ultrathin silicone coating. This indicated that at high cross flow velocities on the shell side, the water permeation flux may be substantially enhanced. No leakage of salt or water was encountered in extended use of these modules in VMD.

The DCMD performances of different modules yielded low values of water permeation fluxes due to four reasons. Since the wall thickness of the hollow fibers was low, there was tremendous heat loss by conduction to the cold distillate; on the other hand in VMD, such losses were very small around 4%. Secondly, due to low fiber internal diameter and very large number of fibers (6000) in Module 5, the distillate flow rate through the fiber bore was low. This reduced the overall temperature difference drastically. Further in the very large cross flow module (Module 5), the ultrathin coating polymer employed was a fluoropolymer having a very low water permeance. In addition, the large brine flow cross section in the module design resulted in very low cross velocities, low Reynolds numbers (around 1) and correspondingly low heat transfer coefficients. Modules made of hollow fibers having larger internal diameter, large wall thickness, high porosity and silicone coating and high cross flow velocities as well as large flow velocities of cold distillate are expected to yield much higher water fluxes in DCMD.

2. Background and Introduction to Potential Solution

Research and development of desalination technologies to increase the availability of cheap and reliable sources of potable water is of significant importance due to the ever increasing population and their needs. Although research and development efforts have focused primarily on existing membrane-based and thermally-driven processes and technologies, there is need for alternative desalination technologies which may potentially be easier to use, cost effective and use energy like low-grade waste heat currently not utilized. Membrane distillation is one such process for desalination.

Membrane distillation (MD) is an evaporation process of a volatile solvent or solute species from a solution (in most cases, an aqueous solution), driven by a difference between its partial pressure over the solution contacting one side of a porous hydrophobic membrane and its partial pressure on the other side of the membrane. When the partial pressure difference through the membrane is created by the direct contacting of a liquid cooler than the feed on the other side of the membrane, the process is called direct contact membrane distillation (DCMD). This is illustrated for a hollow fiber-based process in Figure 1a where the hot brine flows on the shell side of the fiber and the cold distillate flows on the tube side through the fiber bore. When the side of the hollow fiber membrane opposite to the hot brine is subjected to vacuum to offer a partial pressure difference across the membrane, the process is identified as vacuum membrane distillation (VMD). Figure 1b illustrates the VMD process where the hot brine flows on the shell side of the fiber and vacuum is applied on the tube side.

In a MD process, the membrane used must be porous and hydrophobic. Surface tension forces withhold liquids from the pores, and prevent the penetration of the liquid and thus contact between the two liquids in a DCMD process. Generally, the solutions are aqueous and their surface tensions higher than the critical surface tension of the polymer making the membrane. In a DCMD process, the temperature difference, causing a corresponding vapor pressure difference across the membrane, provides the driving force of the membrane distillation process. Evaporation will occur at the solution surface if the vapor pressure on the solution side is greater than the vapor pressure at the condensate surface. Vapors then diffuse through the pores to the cooler surface where they condense. The dependences of mass and heat transport upon different membrane and process parameters involved in membrane distillation have been investigated theoretically (Schofield et al., 1987, 1990a,b; Lawson and Lloyd, 1996; Martinez-Diez and Vazquez-Gonzalez, 1999).

A system of great research interest in MD is the production of fresh water from saline water. The advantages of membrane distillation for water production by such a method are:

(a) it produces high quality distillate;
(b) water can be distilled at relatively low temperatures (30 to 100 ºC) and low pressure (1 atm);
(c) low grade heat (solar, industrial waste heat, or desalination waste heat) may be used;
(d) the water does not require extensive pretreatment to prevent membrane fouling as in pressure-based membrane processes.

Potential disadvantages of the process are:

(a) the water evaporation rate is strongly controlled by the brine side heat transfer coefficient resulting in a relatively low permeate flux compared to other membrane filtration processes such as reverse osmosis (RO);
(b) over an extended time, there is flux decay and distillate contamination due to pore wetting;
(c) uncertain economic cost.

This research has explored two techniques to enhance the potential for the DCMD process. To prevent pore wetting and long-term flux decay, an extremely thin highly water vapor permeable coating of a hydrophobic polymer was applied on the outside surface of microporous hydrophobic polypropylene hollow fibers facing the hot brine to make the membrane essentially nonwettable. The resulting configuration for DCMD is illustrated in Figure 1c. The corresponding configuration for VMD is shown in Figure 1d. Secondly, transverse flow of hot brine over this coated fiber surface was implemented via novel module designs to enhance the brine side heat transfer coefficient, reduce temperature polarization and thereby increase the water vapor flux across the membranes. This research utilized small hollow fiber modules to study the desalination performance and water vapor flux achieved under DCMD conditions. Vacuum membrane distillation using pure water as well as saline water was also carried out extensively to understand better the DCMD performances. Since tube-side flow and transport can be characterized much better than shell-side cross flow, most VMD experiments were done with hot feed flow through the tube-side regardless of whether the fiber had a nonporous coating or not (Figures 1e and 1f). A large module having coated fibers and rectangular cross flow design was utilized to develop preliminary estimates of the water vapor flux in VMD as well as DCMD.

3. Conclusions and Recommendations

1. Numerous VMD and DCMD experiments using a small silicone-coated hollow fiber Module 4 lasting over a cumulative duration of 1000 hours (among them approximately 400 hours for 1wt % or 3wt % brine) without any module washing in between the runs demonstrated that the membrane pores were not wetted by saline water/deionized water at any time. The ultrathin plasmapolymerized silicone coating on the porous polypropylene hollow fiber surface was successful in preventing any pore wetting by water or saline solutions when these solutions were flowing on the coating side.

This conclusion has to be tested in future by an extended run needed to be carried out on a continuous basis over 10 days – 1 month.

2. A water permeation flux of 15 kg/m^2 h was achieved at 91 ^oC in VMD using a parallel flow Module 4 containing silicone-coated fibers and high deionized water velocity through the fiber lumen. Such an experiment has to be carried out in the cross flow mode with the saline water on the shell side. In the same module a water permeation flux of 7 kg/m^2h was achieved at 70 ^oC in VMD using 3 wt% saline water through the fiber lumen. This water flux was also achieved with deionized water.

3. For the DCMD process, larger hollow fibers having much higher wall thickness and high wall porosity have to be used in the module to drastically reduce conductive heat transfer. The flow cross-sectional area in the rectangular crossflow module (for example, Module 5) has to be reduced considerably to increase the cross flow velocity of the hot brine in laboratory experiments. To increase the cold distillate velocity in the fiber lumen and reduce the pressure drop in the cold distillate flow path, the fiber diameters should be significantly larger.

4. The ultrathin hydrophobic water-vapor permeable coatings to be employed in cross flow modules having hollow fibers with larger wall thickness should be of either plasmapolymerized silicone or PDD-TFE. The latter has a very high free volume unlike the fluoropolymer coating employed here in Module 5.

The desired coatings and fibers are available. Due to lack of time and resources in this 1 year project, these modifications could not be implemented.

4. Work Performed

4.1 Experimental Details

4.1.1 Membrane modules

The characteristics of the hollow fibers and the membrane modules are listed in Table 1. Digitized drawings of the radial cross flow Module 3 and the rectangular cross flow Module 5 were not available to us and are therefore provided in the Appendix 1 via scanning. Appendix 1 illustrates the basic Module 5 design as well as a schematic of Module 3. The parallel flow module designs are standard. Appendix 1 also shows the photograph of Module 4.

The original Module 5 received from AMT, Inc., Minnetonka, MN, was only a rectangular channel having coated hollow fibers running across and two open faces. The hollow fibers were well-spaced; the effective length of the fibers was 25.5 cm, the height of the fiber layer was 9.0 cm and its depth was 1.8 cm; other characteristics of the module have been listed in Table 1. We designed a diverging section and a converging section to allow the fluid to flow uniformly in cross flow outside of and perpendicular to the fibers. The diverging and converging sections were two boxes having a shape and cross sectional area equal to that of the flow channel with fibers. On each box, a big hole was opened on one side having the same cross sectional area; 30 smaller holes were uniformly opened on the opposite side. The material used for the channel and the boxes were clear cast acrylic sheet, with reasonable thickness and heat transfer resistance.

With the side having more holes facing the open face of the channel of fibers, two boxes were attached to the channel to constitute the complete device. The hot liquid was allowed to enter one box, then leave the box through the uniformly distributed holes and enter the channel. Then the liquid left the channel through the uniformly distributed holes in the other box and collected in the box and then flowed beyond the box and thus the module. By our special design, there was no free space between the faces of the two boxes and the fiber layer. Therefore, the liquid uniformly and perpendicularly crossed the fiber layer to ensure better heat and mass transfer.

Development of PDD-TFE (perfluoro dimethyl-dioxole-tetrafluoroethylene) coating on Celgard fibers could not be implemented since Compact Membrane Systems Inc., Wilmington, DE, who own the proprietary coating, imposed many restrictions. The issue has been resolved only recently; it was too late for implementation.

4.1.2 Experimental apparatus and procedure

The experimental setups of the DCMD and VMD are schematically shown in Figures 2a and 2b, respectively. Appendix 1 provides a photograph of the experimental setup of Figure 2a. These setups were prepared under Task 2 and Task 3. Appendix 2 provides a summary of the project tasks.

In the experimental setup for DCMD shown in Figure 2a, deionized water or saline water feed was introduced to the fiber lumen side or shell side from a reservoir by a digital Masterflex

peristaltic pump (Model No. 7591-50) at a constant flow rate. The connecting tube was immersed in the water bath before the feed entered the module. A Fisher Scientific temperature controller (Model No. 7305) maintained the bath temperature at a given value and thus maintained a constant entrance temperature for the hot feed. Outside the membrane module, the feed was circulated to the feed reservoir and was re-warmed.

Deionized water was introduced as a cooling liquid on the other side of the module from a reservoir by another digital Masterflex peristaltic pump (Model No. 7518-10) at a constant flow rate. The connecting line was immersed in the water bath before the feed entered the module. A Haake temperature controller (Model No. A81) maintained the bath temperature at a given low temperature and thus maintained a constant entrance temperature for the cooling water entering into the module. The inlet and outlet temperatures of the hot feed and the cold water were measured by four thermocouples. The feed-in and feed-out tubings to the module were each fitted with a three-way valve for sampling. The electrical conductivity or the salt concentration of the samples was measured by a conductivity meter (Model No. 115, Orion Research, Beverly, MA).

When the readings of the four inlet and outlet temperatures reached constant values, the volume reduction in the feed reservoir and the volume increase in the cooling water reservoir were used for the calculation of water permeation flux through the membrane under the given experimental conditions. Water permeation flux was calculated from the following relation:

$$\text{Water permeation flux } (\frac{\text{kg}}{\text{m}^2\ \text{hr}}) = \frac{\text{vol. of water transfer (l)} \times \text{density of water (kg/l)}}{\text{membrane area (m}^2) \times \text{time (hr)}} \quad (1)$$

In the experimental setup for VMD shown in Figure 2b, deionized water or saline water was introduced as a feed to the fiber lumen side or shell side from a reservoir by a digital Masterflex peristaltic pump at a constant flow rate. The pipeline was immersed in the water bath before the feed entered the module. A Fisher Scientific temperature controller maintained the bath temperature at a given level and thus maintained a constant entrance temperature for the hot feed. The exits of the other side of the module were connected with an evacuation system to maintain vacuum by a Welch GEM 1.0 vacuum pump. The vacuum was monitored by a J-KEM Scientific digital vacuum regulator (model 200) and controlled by means of a needle valve attached to the bypass loop of the regulator at a preset pressure within ± 1 mm Hg. A glass vacuum trap (Lab Glass Inc., Vineland, NJ) immersed in a liquid N_2 well (Dewar flask, Lab Glass Inc.) or salt water-ice mixture and connected in series to the vacuum pump was used to collect the permeate vapor. There were two such vacuum traps.

The weights of each vacuum trap were taken before and after permeate collection for calculation of water flux. Permeate vapors were collected for a fixed interval of time in the attached vacuum trap. This trap was then isolated from the system for sampling purposes by a set of two three-way ball valves while the stand-by vacuum trap was brought online. This was achieved by switching the vacuum pump to the stand-by trap, by means of one of the three-way ball valves attached between the vacuum pump and the vacuum trap. After stabilization of the vacuum in the stand-by trap, it was immersed in a new liquid N_2 well. At the precise changeover time, the second three-way ball valve, attached between the hollow fiber module shell side and

the vacuum trap, was switched over to the stand-by vacuum trap thus bringing it online. Water permeation flux was calculated from the following:

$$Water\ permeation\ flux\ (\frac{kg}{m^2\ hr}) = \frac{wt.\ of\ condensed\ water\ (kg)}{membrane\ area\ (m^2) \times time(hr)} \qquad (2)$$

The isolated vacuum trap was then removed from the liquid N_2 well and its temperature was allowed to rise up to room temperature. The electrical conductivity or the salt concentration in the samples was measured by a conductivity meter (Model No. 115, Orion Research, Inc., Beverly, MA). In various VMD and DCMD experiments, either deionized water, 1 wt% or 3 wt% solution of NaCl in water was employed as hot feed; deionized water was used as the cold distillate in DCMD experiments.

A system was also established for the measurement of the water vapor permeance of the nonporous coating on the microporous substrate using a gas permeation apparatus. The feed and sweep flow rates were controlled using electronic mass flow transducers and multiple flow controller (Model 8274, Matheson, Horsham, PA). Dry N_2 was presaturated by bubbling it through a cylinder filled with deionized water. The presaturated N_2 was introduced into the module via the lumen or the shell, while the sweep gas, dry N_2, was passed through the other side of the membrane. The outlet flow rates of the feed and sweep gas were measured using two soap bubble flow meters. The humidities of the feed inlet and the feed outlet were measured by humidity probes (Model HMP 31UT, Vaisala, Woburn, MA). Steady state readings of the humidity were used for the calculation of water vapor permeance.

4.2 Experimental Results and Discussion

4.2.1 VMD experiments (Task 3)

Each membrane module having different kinds of hollow fibers or different module configurations was tested by VMD experiments. The effects of the inlet temperature, presence of NaCl in the feed, volumetric flow rate of the feed (or the linear velocity), the module flow configuration (parallel or cross flow), and the feeding mode (shell side or lumen side) on the water permeation flux and the outlet temperature are illustrated in Figs. 3 – 12. Note when the hot feed is flowing through the lumen, then VMD configurations relevant are described in Figures 1f (coated fiber) and 1e (porous fiber).

As illustrated in Figs. 3 - 5, as the temperature of the hot deionized water feed was increased, the water permeation flux was increased. The water permeation flux also linearly increases with the water feed flow rate or the linear velocity through the lumen side of the parallel flow Modules 2, 1 and 4 respectively. Note, of these modules, only Module 2 (Figure 3) has porous fibers and has a higher slope of flux with velocity; this shows that the coating in Module 1 (Figure 4) and Module 4 (Figure 5) provide some resistance to water vapor transfer.

The effect of much higher flow rates on the water flux for Module 4 is illustrated in Fig. 6. Note that the flow velocities in Fig. 6 are much higher than in any other experiments so far. This

has increased the hot feed side heat transfer coefficients considerably. From Fig. 6, it can be also seen that the water permeation flux for 70 ^{o}C feed can be as high as 7 kg/m^{2}h, which is, however, comparable to the results for hollow fiber membranes reported in the literature (Bandini et al., 1992). This figure also has many results for hot brine feed containing 3 wt% salt. It appears that the water permeation flux was not apparently influenced much by the addition of the salt to the feed, as concluded in the literature (Lawson and Lloyd, 1996). Note that this high flux (7 kg/m^{2}h) was achieved at 70^{o}C. At higher temperatures, we expect that the flux would be a few times higher as will be shown later.

The effect of the silicone coating on the water permeation flux is shown for Modules 1 (coated), 2 (porous) and 4 (coated) in Fig. 7 as a function of the residence time of the feed fluid. Note as the linear velocity increases, the residence time decreases. It can be seen that the porous substrate membrane in Module 2 resulted in the highest permeation flux. Regardless of whether the coating was a completely nonporous one with a plasmapolymerized silicone coating of thickness ~1μm on the outer surface (Module 1) or with a plasmapolymerized silicone coating with anywhere from 5-15 Å openings on the outer surface (Module 4), the water permeation fluxes were significantly reduced due to the presence of the coatings. Note that the flow velocites here are very low compared to those achieved in Fig. 6. Even so, the water permeation flux through the membrane (and the coatings) is significant as seen from the significant temperature drop through the module (Fig. 8).

Module 2 having parallel flow was also used for the operation when the feed was flowing through the shell side of the module; as seen in Fig. 9, the water permeation flux was much lower than that when the deionized water feed was flowing through the lumen side of the module due to the maldistribution of the flow in the shell side due to bypassing or channeling near the wall.

The cross flow membrane modules were also tested for VMD. As seen in Fig. 10, the water permeation flux through Module 5 having rectangular cross flow and coated membranes was much lower than that through the radial cross flow Module 3, a modified blood oxygenator having fibers without any coating, for a similar water residence time in the modules; the permeation flux when the feed was flowing through the shell side of Module 5 having coated fibers was very close to that when the feed was flowing through the lumen side for identical volumetric flow rates. Furthermore, as illustrated in Fig. 11, the outlet temperatures when the feed was flowing on the shell side of Module 5 having coated membranes were only slightly lower than the corresponding inlet ones, as compared to the results when another coated membrane was used (see Figure 8 for Module 4). The results obtained from the large module (Module 5) were further compared to the results obtained from the small module (Module 4) in Figure 12. It can be seen that the water flux through the large module was much lower than that through the small module (Module 4) under similar experimental conditions.

We have been in communication with Applied Membrane Technologies (AMT), Minnetonka, MN, regarding the nature of the coatings in Module 5. Only recently we came to know that the coating on the outside of the hollow fibers used in Module 5 was quite different from the silicone coating on the outside of the hollow fibers used in Module 4. The coating used in Module 5 was a fluoropolymer having a much higher resistance to water vapor transport than silicone coating. However, this large cross-flow module was quite costly since it was

developmental; we obtained it essentially as a gift. A similar module having a silicone coating of the type used in Module 4 would have performed better.

Using the thermodynamic properties of water, we can calculate the membrane distillation efficiency η as

$$\eta = F\,\Delta H / V_{feed}\,C_p\,\Delta T \qquad (3)$$

Here, η is the heat transfer efficiency, F is the water permeation flux, ΔH is the evaporation enthalpy of water, V_{feed} is the flow rate of the feed, C_p is the specific heat capacity of feed, and ΔT is the temperature drop through the module. We found that in a VMD process, whether a cross flow or a parallel flow module was used, or the feed was passed on the lumen side or the shell side, the heat transfer efficiency was as high as ≥96%. Further the highest water vapor fluxes obtained was around 15 kg/m^2h at a feed hot water temperature of around 90°C (Figure 12 for Module 4). Obviously at higher temperatures we can expect this flux to go up to 20-30 kg/m^2h.

These high water fluxes obtained in Module 4 at higher temperatures (70 –91 °C) were achieved only at high lumen velocities. The lumen diameter based Reynolds number for Module 4 had a maximum value of 127. It is well known that cross flow yields much higher heat transfer coefficients at comparable Reynolds numbers. Therefore, it is expected that a cross flow module having fibers used in Module 4 will yield much higher water vapor fluxes in VMD at comparable brine side Reynolds numbers on the shell side.

4.2.2 DCMD experiments (Tasks 2 and 5)

A simple parallel-flow hollow fiber module having the shell-and-tube configuration, namely, Module 4, was first used for the DCMD test. Experimental results are shown in Figs. 13 and 14. Regardless of whether the deionized hot water was fed through the lumen side or the shell side of the module in the DCMD operation, the water permeation flux through the membrane (Module 4) was extremely low as indicated in Fig. 13 when compared to the water permeation flux obtained by vacuum membrane distillation (VMD) in the same module as shown in Fig. 6 and Fig. 12. We should note that, when 3 wt% saline water was used as the hot feed on the shell side, the performance was identical to that with deionized water. The question is why so low a water flux. By a simple heat balance calculation, we found that more than 80% of the heat exchange as a result of the temperature drop in the hot feed was transported to the cold water (Figure 14). Such a low mass transport efficiency in the DCMD process compared to that in the VMD process may be attributed to the maldistribution of the fluid flow, temperature polarization in the shell side, and a great deal of conductive heat transfer. Module 4 fibers have a small diameter, not too high a wall thickness, and the runs did not have a high enough flow rate through the lumen. As a result, the conductive heat transfer was substantial. This reduced the ΔT between the two fluids and therefore the vapor pressure driving force. Module 4 has parallel flow which is also highly susceptible to bypassing on the shell side.

We have further tested Module 3 having radial cross flow. The experimental DCMD results are shown in Figure 15 and Table 2. Surprisingly, the water permeation flux through the porous

Celgard membrane of Module 3 was very low, even lower than that obtained in the simple shell-and-tube module 4 having silicone coated fibers (see Figure 13). However, it can be seen that the outlet temperature of the feed is very close to the inlet temperature of the cold water and the outlet temperature of the cold water is very near the inlet temperature of the feed. In this module (see Appendix 1 for a schematic of the module), the shell side fluid was fed into the central tube in the module, passed over the fiber surface in a radial cross flow mode; the fluid was then collected near the wall of the shell and exited from the module. We can conclude that such an operation offered a countercurrent mode of heat transfer for the shell fluid and the lumen fluid.

On the other hand, when the shell side fluid was fed from the exit of the module, i.e., the fluid was passed over the fiber outside surface and then was collected into the central tube and the exit from the module, the device operated in a co-current mode; one notices that because the outlet temperature of the shell side hot feed is quite near to the outlet temperature of the lumen side cooling water (see Table 2), the water permeation flux of 0.123 g/m^2h was lower than that obtained by countercurrent operation (see Figure 15).

As reported in literature (Drioli et al., 1987; Schofield et al., 1987; Fane et al., 1987; Schneider et al., 1988), the water permeation fluxes for DCMD using hollow fiber modules of shell-and-tube configuration were in the range of 1.7 –17 kg/m^2h under similar experimental conditions, when the hollow fibers with thick wall were used; typical wall thickness was 150 – 400 μm. In comparison, the wall thickness of the membranes used in our research was typically 25 μm. The conductive heat transfer rate through the thinner membrane was certainly much higher than that through the thick walled membranes. Further, the thick hollow fibers reported in the literature usually had higher porosity, larger average micropore diameter, and thus smaller tortuosity than the thin ones. This meant that a larger effective diffusion coefficient for water vapor within the micropores in the thicker wall than that in the thinner one. Also this means a smaller effective thermal conductivity in the thicker wall, due to the larger porosity and thicker wall than that in the thin wall. As a net result, hollow fibers having a smaller diameter may offer a much lower membrane distillation efficiency as defined by eq. (3) than what is achievable with a fiber having a larger diameter. We have to mention that the thin coating also offers an additional resistance for mass transport through membrane. The reduction of water permeation flux due to the presence of the coating became more obvious when Module 5, made from fibers having a fluoro- copolymer coating, was used.

Module 5, a large rectangular cross flow membrane module having 6,000 coated hollow fibers, was further tested for DCMD experiments. Some typical experimental results are listed in Table 3. The water permeation flux was quite low due to the resistance from the highly hydrophobic coating as well as considerable conductive heat transfer. In addition, the cross flow cross sectional area was 25.5 x 9 = 225 cm^2; at a flow rate of, say, 3000 ml/min, the flow velocity entering the fiber bed will be only around 12 cm/min. At the location of the fibers, it will be higher by a factor of 2 (say). The Reynolds number corresponding to this value (~1.55) is far smaller than what has been used in VMD process for Module 4 (namely 3.6 to 127) and Module 5, namely, 24 to 48 (Figs. 6 and 12). Although an order of magnitude higher transfer coefficients are achieved in cross flow compared to parallel flow at the same velocity, the cross flow velocities used here were very small.

4.2.3 Vapor permeation experiments (Task 4)

Module 4 made from silicone coated fibers was tested in the vapor permeation mode. The permeation flux of N_2 was first determined by measuring the lumen and shell side outlet flow rates as dry N_2 was flowing through the lumen of the module and one exit of the shell was sealed. The temperature was controlled at the ambient temperature of 22.5 ^oC; higher temperatures were not tested because of possible condensation of the liquid water in the pipelines and the module. When the inlet pressure was controlled at slightly higher than atmospheric pressure, the lumen inlet flow rate, the lumen outlet flow rate and the shell outlet flow rate were 45 ml/min, 25 ml/min and 28 ml/min, respectively. On the other hand, when Module 2 was tested for the same purpose under identical experimental conditions, the lumen outlet flow rate was near zero compared to the shell outlet flow rate. This means that compared to the porous substrate membrane used in Module 2, the coating offers an additional resistance; the resistance is, however, not quite high even to a less permeable gas N_2.

In additional vapor permeation experiments where humid N_2 was flowing through the lumen of the module and dry N_2 was flowing through the shell side countercurrently or cocurrently, we found that for the same lumen inlet flow rate, the lumen outlet flow rate and the lumen outlet humidity were not influenced by the shell inlet flow rate even when the flow rate of dry N_2 in shell was much higher than the flow rate of humid N_2 in the lumen. The variation of lumen (feed) outlet relative humidity is illustrated as a function of inlet flow rate in Fig. 16.

The permeability of water through Module 4 is illustrated in Figure 17. The water permeabilities from VMD experiments in Figure 5 are also included here for comparison. Even though the bulk flow of the feed gas through the module was not considered in the calculation of the permeability, the vapor permeability of water at 22.5 ^oC by vapor permeation was much lower that those obtained by VMD at higher temperatures. Low diffusivity of water vapor at low temperature is the likely explanation. Another important reason is that when one side of the module was evacuated, the diffusivity of the vapor in the micropores drastically increased in spite of the diffusion mechanism (Schofield et al., 1990a). Furthermore, Poiseuille flow was responsible for a significant contribution to the vapor transport through the membrane during the VMD process due to the large pressure difference across the membrane.

4.2.4 Salt rejection

In all VMD and DCMD experiments, either deionized water, 1 wt% or 3 wt % solution of NaCl was used as the feed. In the DCMD experiments, deionized water was used as the cooling water. The concentration of any salt in the deionized water was less than 1ppm. For each and every DCMD experiment, we measured both the conductivity and the salt concentration in the cooling water (distillate); the concentration in the distillate was always less than 1 ppm, without any exception.

4.2.5 Stability test (Tasks 2 and 3)

As mentioned in the above section, all membranes used have essentially 100% salt rejection. Module 4 made of hollow fibers having a thin plasmapolymerized silicone coating has

been used since the end of March, 2000; Module 5 made of hollow fibers having a thin microporous fluoropolymer coating has been used since the end of September, 2000. Up to now, they were continually used for VMD and DCMD tests; Module 4 was used approximately for more than 1,000 hrs. Under identical experimental conditions used in earlier experiments with Module 4 for VMD and DCMD, Module 4 having fibers with silicone coating recently gave essentially the same performances, except that the pressure drop when the feed was passing the lumen side of the module was slightly increased (by 10 – 20%). On the other hand, for a similar period, porous membranes demonstrated a reduction of more than 20% in the water permeation flux (Banat and Simandi, 1994).

Appendix 3 provides the Tables of data collected in this work.

5. Analysis of Results and Commercial Viability of the Project

Two items are of great importance when analyzing the experimental results.

1. Did the hydrophobic coating prevent salt intrusion into the membrane pore and prevent membrane wetting?
2. How do the experimentally obtained water permeation flux values compare with the level desired for economic operation?

In so far as question 1 is concerned, the results from the VMD experiments as well as DCMD experiments indicated that the hydrophobic coating on the fibers in Module 4 and Module 5 did not permit any salt intrusion into the fiber pores. The experiments were done without any module washing after a given run, which may last 6 – 9 hours. Although the cumulative duration of such experiments for Module 4, for example, was around 1000 hours, only about 400 hours used saline water. To settle the question of prevention of pore wetting by the coating conclusively, however, will require an experiment running continuously for 10 –30 days. This was not contemplated in the present project. In addition, only two experiments were done at temperatures beyond 75 ^{o}C, namely, at 80 ^{o}C and 91 ^{o}C (Figure 12). The continuous experiments that may be carried out in a future project should use 85 – 90 ^{o}C to determine whether the behaviors of the substrate polymer and the coatings are going to be affected by continued use at the higher temperatures.

The VMD-based water permeation flux obtained at 70 ^{o}C from Module 4 (having parallel flow) at a high feed velocity through the fiber lumen (35 cm/s) was around 7 kg/m^2 h (Figure 6). The vapor pressure of water at 91 ^{o}C over brine or pure water will be more than double of that at 70 ^{o}C. Thus, a water permeation flux of 15 – 20 kg/m^2 h can be achieved easily. Figure 12 proves it; at 90 ^{o}C the VMD flux at the same lumen velocity is 15 kg/m^2-h. If one can use cross flow on the outside of the fibers, it is well known that the transfer coefficient at a given flow velocity can be 7 –10 times larger than in parallel flow. Therefore, cross flow velocity of around 5 – 7 cm/s will yield very high transfer coefficient which will lead to VMD-based water permeation fluxes of 30 – 70 kg/m^2 h.

The two cross flow modules studied in the project, namely, Module 3 and Module 5, did not yield high water permeation fluxes in DCMD. We ascribe these to a number of reasons. First, the fluoropolymer coating on Module 5 is likely to have a very low water permeation characteristics. Since this coating was totally new and the module size was very large, moisture permeation experiments in the gas phase could not be done. Smaller modules have to be tested in the vapor permeation mode to judge the nature of the coating. Second, the cross flow velocity in Module 5 was quite small. Given the large cross section of the module provided by the manufacturer, the cross flow velocities achieved in the present experimental setup were very low. Third, the conductive heat transferred in this module as a fraction of the total heat transferred from the hot brine was very high. We have to select hollow fibers having much thicker and more porous walls to reduce the conductive heat loss. Further, the flow rate through the fibers has to be much larger so that ΔT between the two fluids remains high without high pressure drop. This will require larger diameter fiber bores. The same problem was encountered with Module 3. In fact Module 3 (Medtronics, Inc.) seems to have been designed with extremely efficient conductive heat transfer capability (Table 2).

Obviously, the DCMD-based water permeation fluxes achieved in this 1-year project are very low. The VMD-based water permeation fluxes are in a reasonable range and with a few changes can be brought up to 30 – 70 kg/m^2 h range. To bring the DCMD-based water permeation fluxes up to the economic level of 30 – 70 kg/m^2 h range desired for economic operation, a number of steps have to be taken in future. These have been identified in the previous paragraph.

6. References

Bandini, S., C. Gostoli, and G. C. Sarti, Separation efficiency in vacuum membrane distillation, J. Membr. Sci., 73, 217-229, 1992.

Banat, F. A. and J. Simandi, Theoretical and experimental study in membrane distillation, Desalination, 95, 39-52, 1994.

Drioli, E., Y. Wu, and V. Calabro, Membrane distillation in the treatment of aqueous solutions, J. Membr. Sci., 33, 277-284, 1987.

Fane, A. G., R. W. Schofield and C. J. D. Fell, The efficient use of energy in membrane distillation, Desalination, 64, 231-243, 1987.

Lawson, K. W., and D. R. Lloyd, Membrane distillation, II. Direct contact MD, J. Membr. Sci., 120, 123-133m 1996.

Martinez-Diez, L., and Mi. I. Vazquez-Gonzalez, Temperature and concentration polarization in membrane distillation of aqueous salt solutions, J. Membr. Sci., 156, 265-273, 1999.

Schneider, K., W. Holz, R. Wollbeck, and S. Ripperger, Membranes and modules for transmembrane distillation, J. Membr. Sci., 39, 25-42, 1988.

Schofield, R. W., A. G. Fane, and C. J. D. Fell, Heat and mass transfer in membrane distillation, J. Membr. Sci., 33, 299, 1987.

Schofield, R. W., A. G. Fane, and C. J. D. Fell, Gas and vapor transport through microporous membrane. I. Knudsen-Poiseuille transition, J. Membr. Sci., 53, 159-171, 1990a.

Schofield, R. W., A. G. Fane, and C. J. D. Fell, Gas and vapor transport through microporous membrane. II, J. Membr. Sci., 53, 173-185, 1990b.

7. Tables

Table 1. Details of the hollow fibers and the membrane modules used

Particulars	**Module 1**	**Module 2**	**Module 3**	**Module 4**	**Module 5**
Membrane type	Celgard X-20	Celgard X-20	Celgard X-30	Akzo, Netherlands	Akzo, Netherlands
Coating	silicone*	none	none	silicone**	fluoropolymer
No. of fibers	300	78	unknown	300	6,000
Membrane porosity	0.40	0.40	0.40	0.60	0.60
Fiber O.D., μm	290	290	260	305	305
Fiber I.D., μm	240	240	210	200	200
Packing fraction	0.20	0.20	unknown	0.30	0.27
Effective fiber length, cm	20.5	32.0	unknown	17.1	25.5
Effective area, cm^2	547	227	2323	491	9600
Shell side flow mode	parallel	parallel	radial cross flow	parallel	rectangular cross flow
Fabricated at	NJIT	NJIT	Medtronics Inc., Minneapolis, MN	AMT Inc., Minnetonka, MN	AMT Inc., Minnetonka, MN

* Silicone coating via plasma polymerization: thick coating; coated fiber obtained from AMT, Inc.

** Silicone coating via plasma polymerization: ultrathin coating having 5 - 15Å pores specified by us; manufactured by AMT Inc.

Table 2. Outlet temperature variation with the feed (1 wt% saline water) and cooling water (deionized water) inlet temperature when the feed and the cold water were passed through the shell side and lumen side respectively of the radial cross flow Module 3

Flow mode	V_{feed}, ml/min	V_{cold}, ml/min	$T_{feed\text{-}in}$, ^oC	$T_{feed\text{-}out}$, ^oC	$T_{cold\text{-}in}$, ^oC	$T_{cold\text{-}out}$, ^oC
Countercurrent	60	60	40.4	32.1	30.0	37.3
Countercurrent	60	60	50.0	38.7	38.0	47.9
Countercurrent	60	60	60.0	42.0	38.6	55.4
Countercurrent	160	160	40.0	50.0	28.6	37.4
Countercurrent	160	160	50.0	38.7	38.4	47.9
Countercurrent	160	160	60.0	45.5	43.0	55.8
Cocurrent	160	160	50.0	38.3	30.0	40.8

Table 3. DCMD performance of Module 5 as the hot feed was passed through the shell side in rectangular cross flow over the fibers (feed: 1 wt% saline water; cold water: deionized water)

$T_{hot\text{-}in}$, ^oC	$T_{hot\text{-}out}$, ^oC	$T_{cool\text{-}in}$, ^oC	$T_{cool\text{-}out}$, ^oC	V_{feed}, ml/min	V_{cold}, ml/min	Permeation flux, g/m^2h
38.8	35.7	31.7	38.2	1880	800	24.0
39.1	36.1	30.1	38.2	1880	640	40.0
40.3	36.8	30.8	38.5	1880	765	28.0
50.0	42.3	28.4	45.6	1880	800	67.0
50.0	42.3	28.4	46.4	1880	780	66.7
50.0	40.6	23.7	43.4	1880	780	80.0
50.0	44.6	20.4	40.8	1880	800	90.0
46.9	39.0	18.8	43.5	1880	800	71.0
50.4	43.8	21.9	48.8	1920	520	80.0
51.0	43.7	19.2	48.2	1920	520	83.0
47.4	41.5	20.1	45.4	2800	1600	122.0

8. Figures

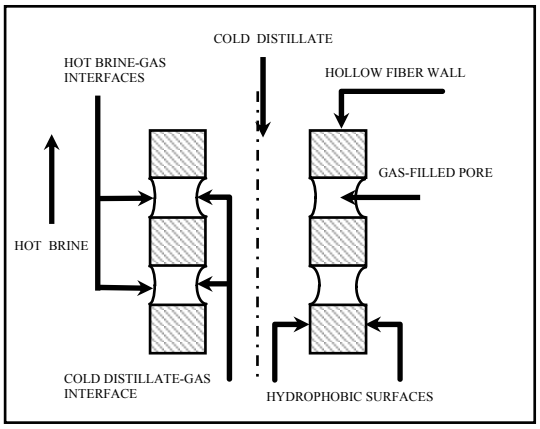

Fig. 1a. Conventional direct contact membrane distillation

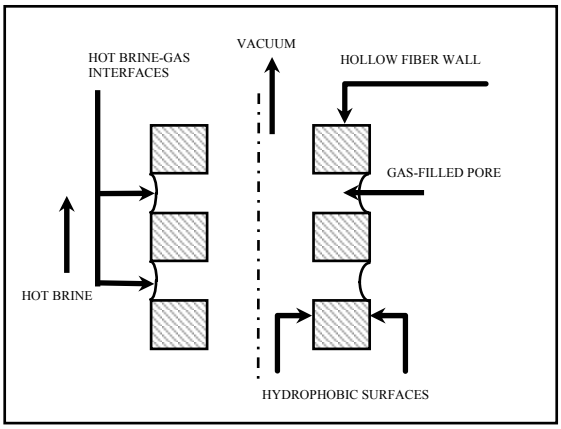

Fig. 1b. Conventional vacuum membrane distillation

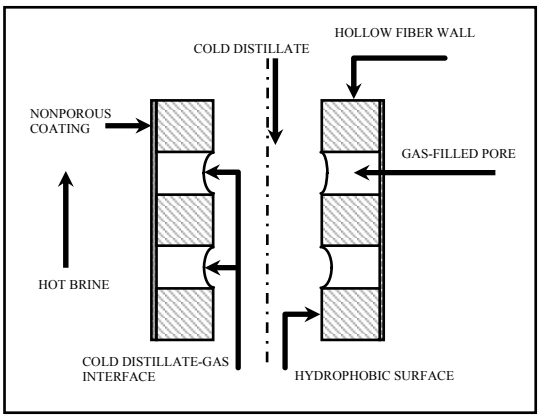

Fig. 1c. Suggested direct contact membrane distillation

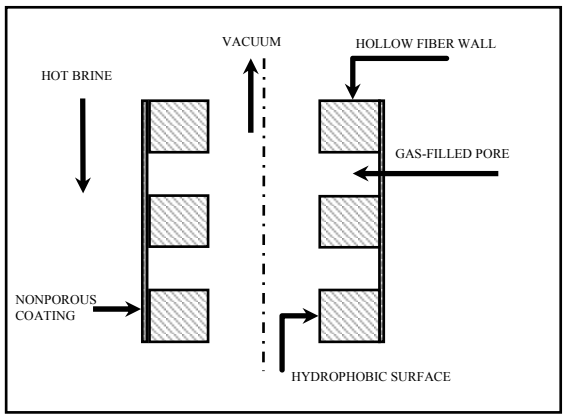

Fig. 1d. Suggested vacuum membrane distillation

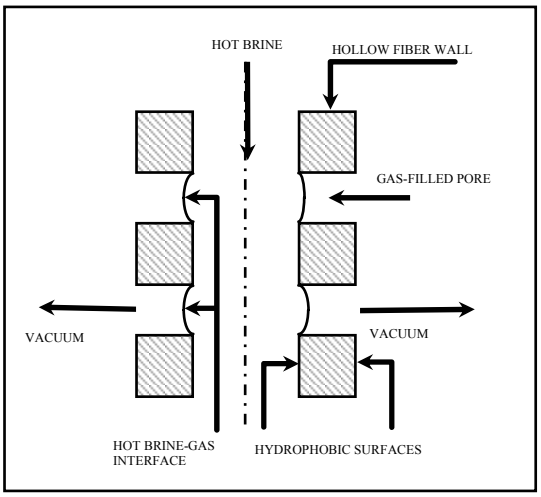

Fig. 1e. Conventional vacuum membrane distillation with hot Brine in lumen

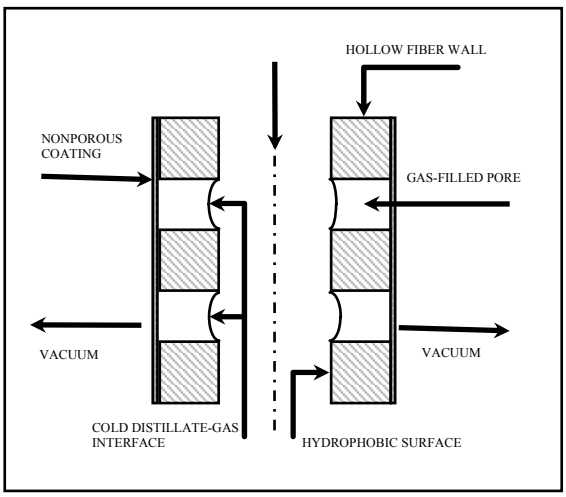

Fig. 1f. Vacuum membrane distillation with hot brine in coated fiber lumen

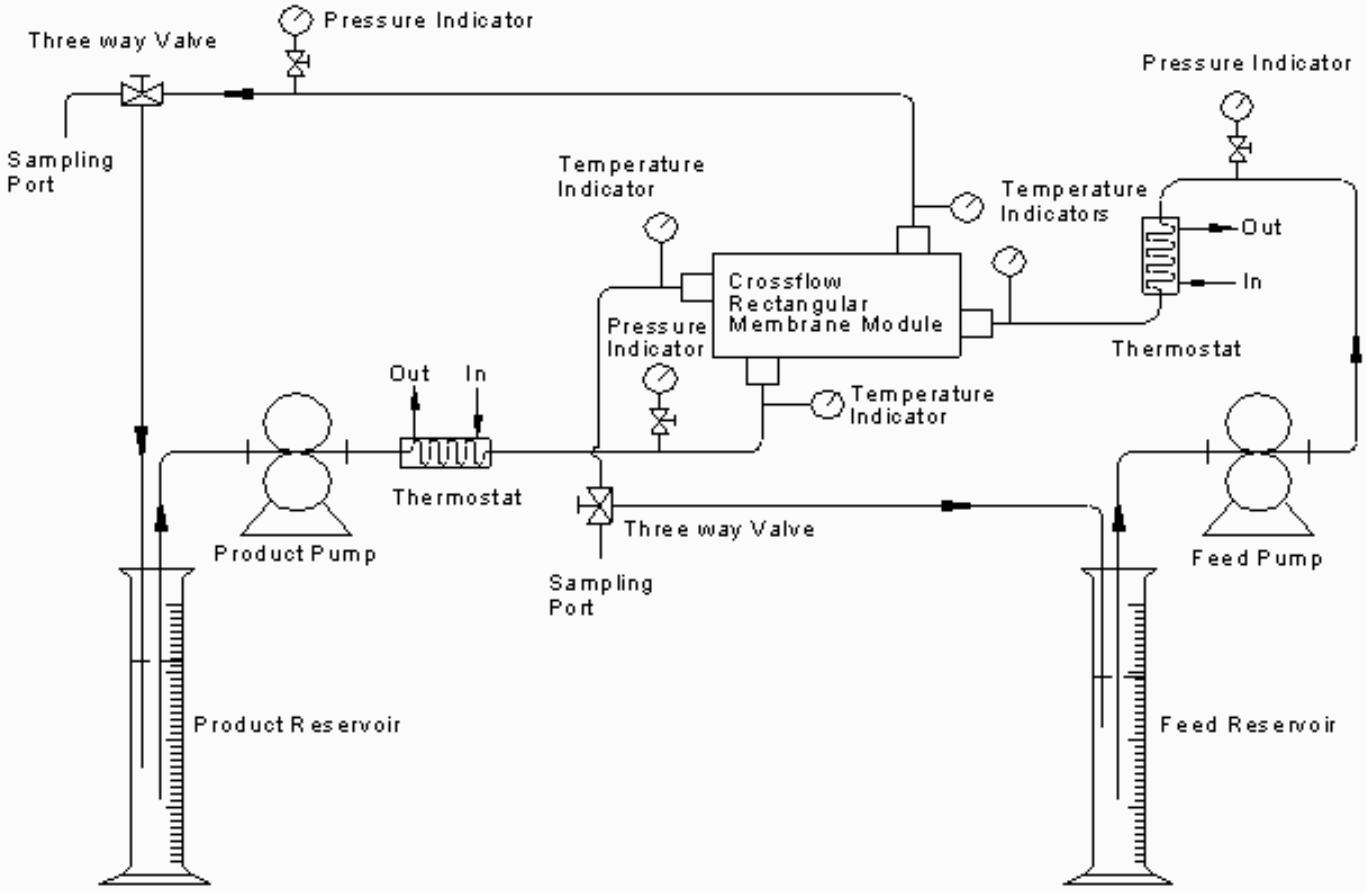

Figure 2a. Experimental setup for DCMD process

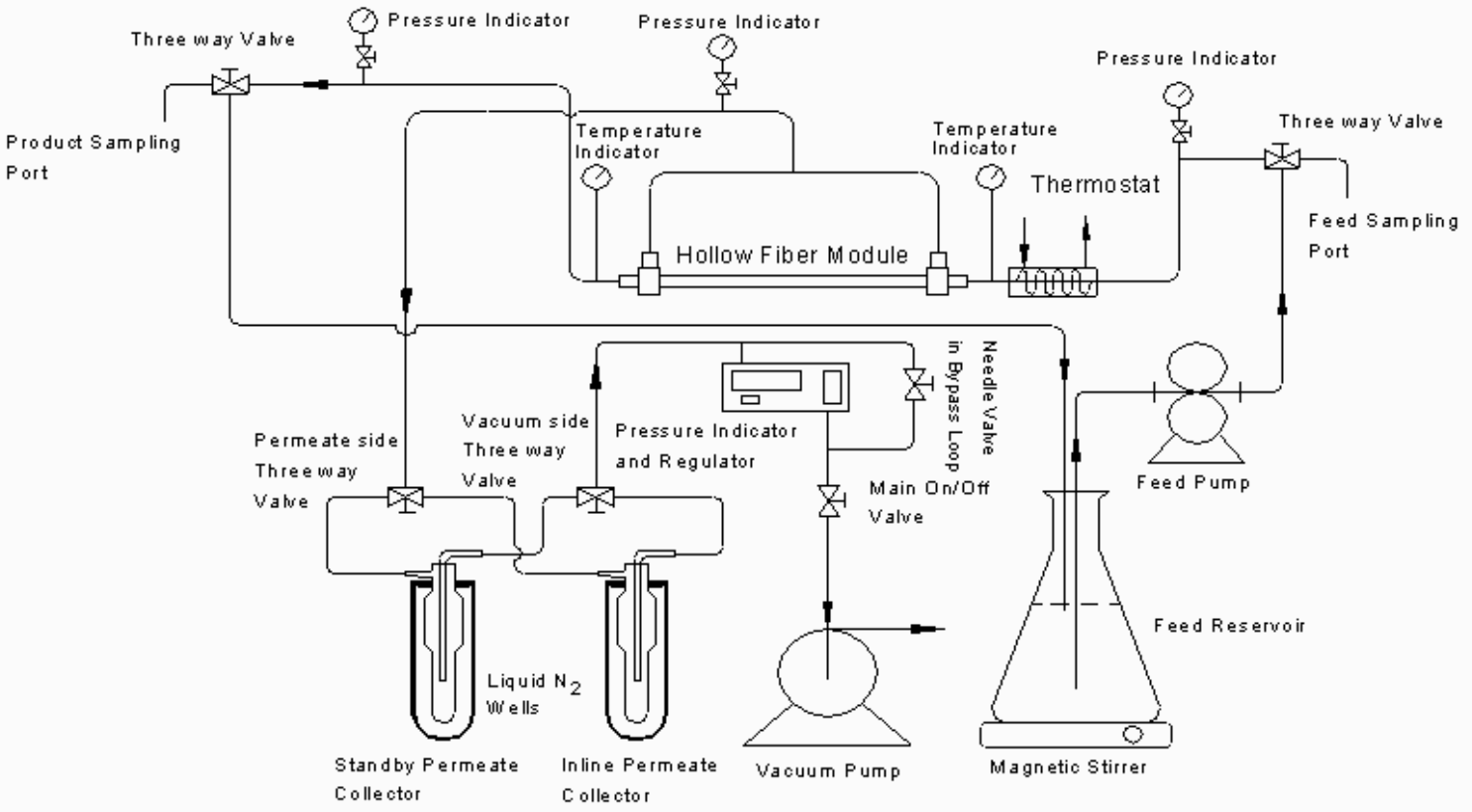

Figure 2b. Experimental setup for VMD process

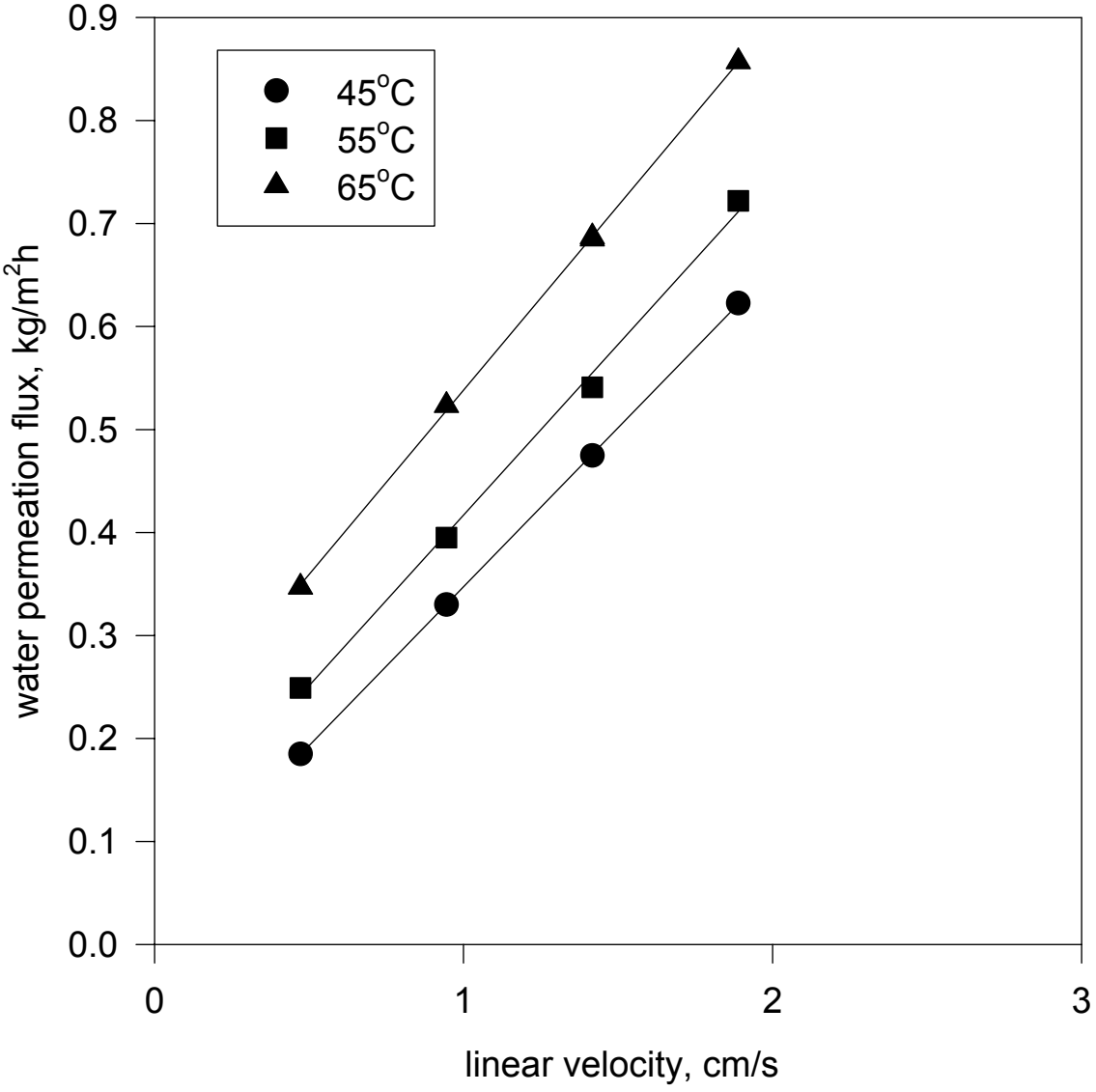

Figure 3. VMD: Variation of water permeation flux with water velocity when water was flowing through the lumen of hollow fiber module at various temperatures (Module 2 having porous fibers used; P_{shell}=15 Torr; deionized water used as feed)

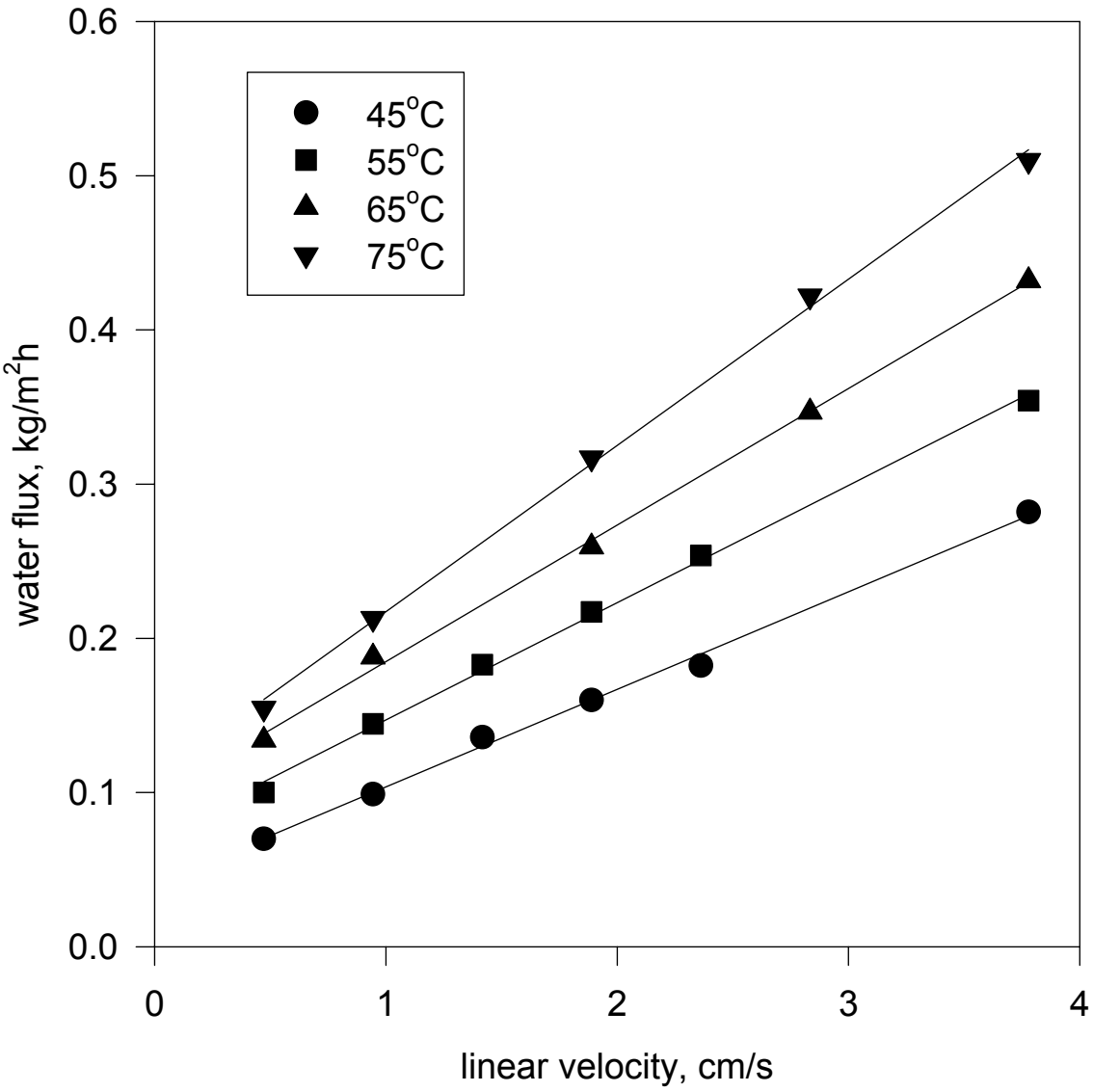

Figure 4. VMD: Variation of water flux through the membrane with water velocity when feed was flowing through the lumen of hollow fibers at various temperatures (Module 1 having silicone coated fibers; deionized water as feed; P_{shell}=15 Torr)

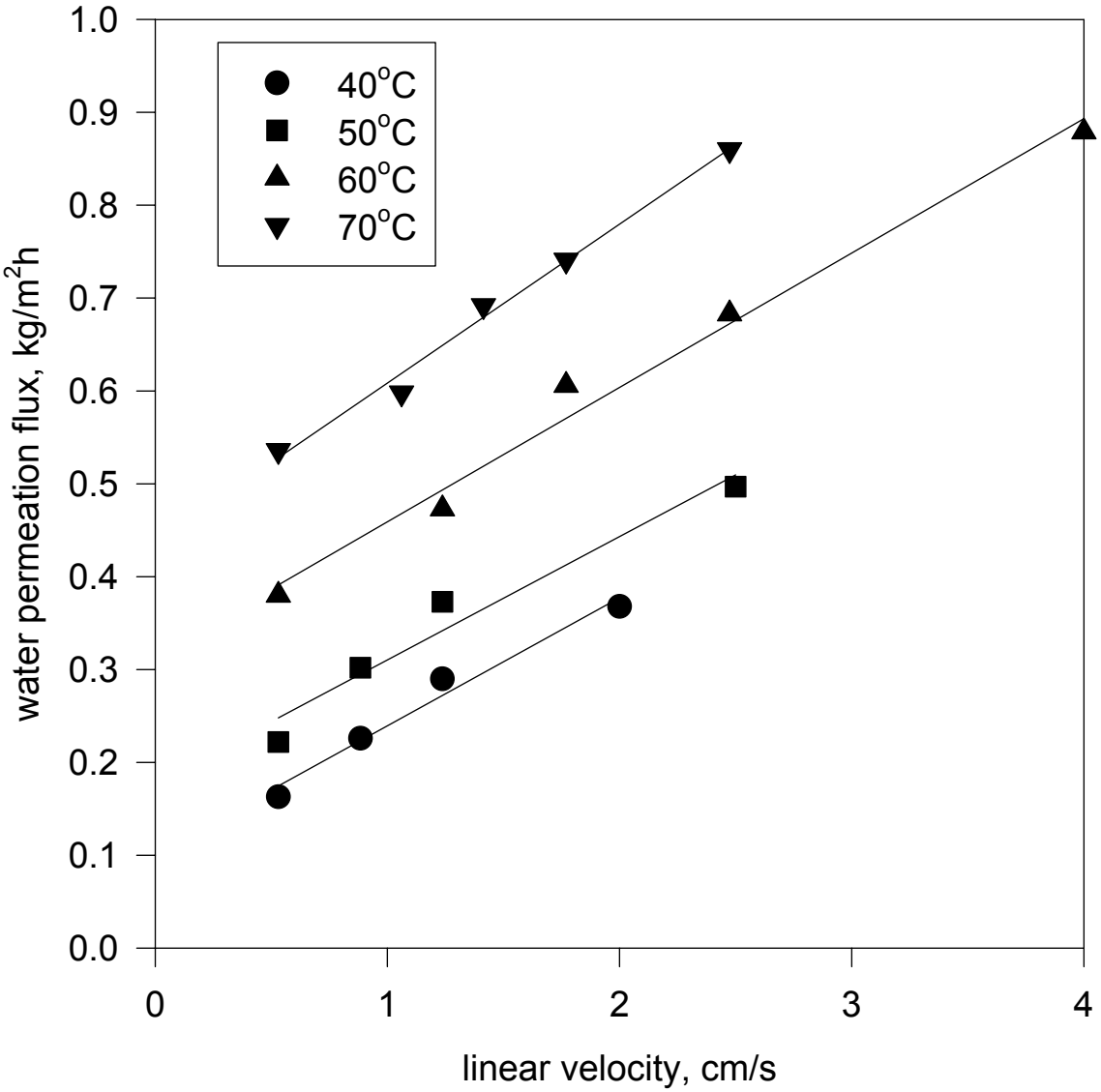

Figure 5. VMD: Variation of water permeation flux with water velocity when feed was passed through the lumen of hollow fibers at various temperatures (Module 4 having coated fibers; deionized water used as feed; P_{shell}=15 Torr)

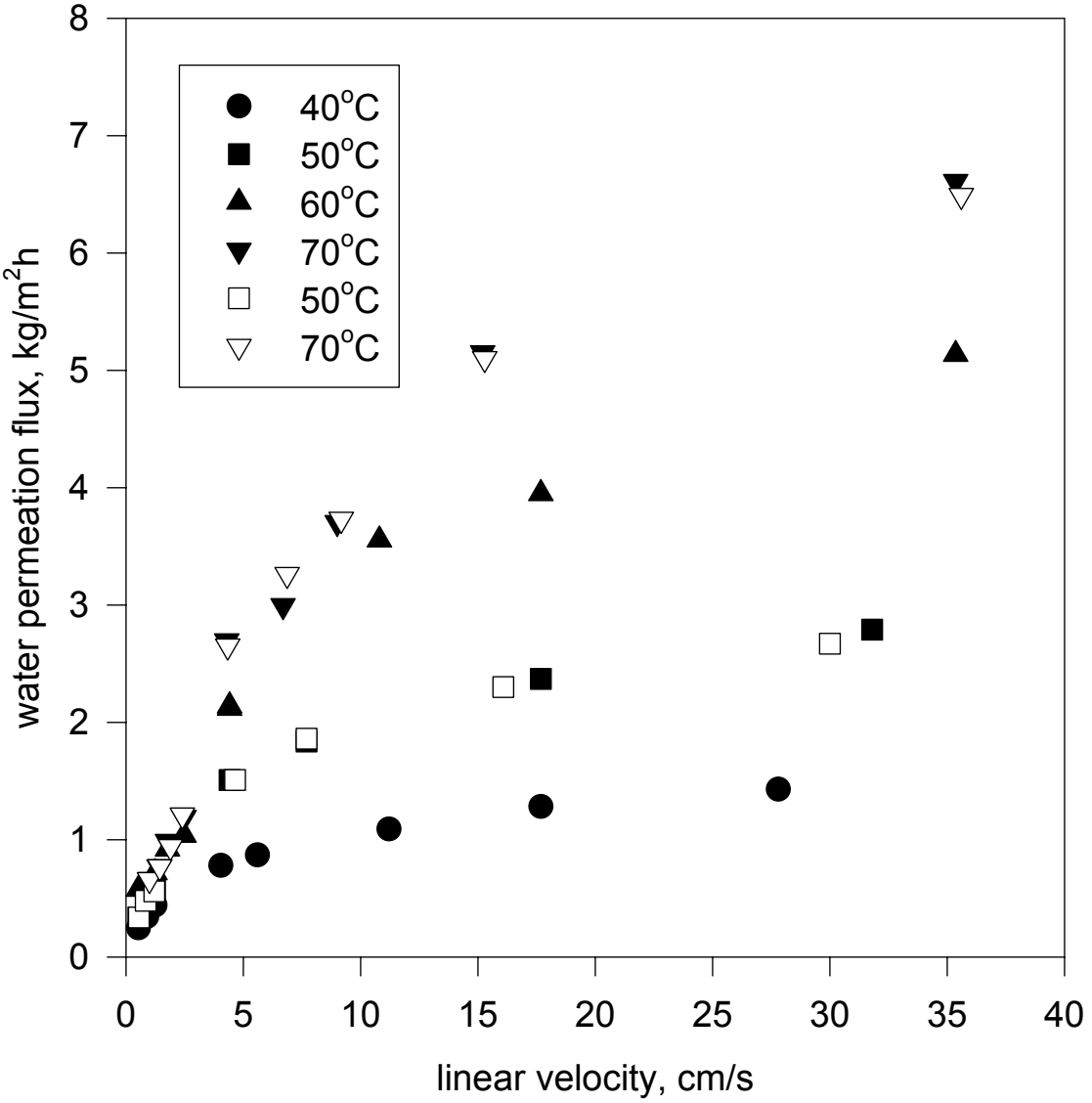

Figure 6. VMD: Variation of water flux with water velocity when feed was passed through the lumen of hollow fibers at various temperatures (Module 4; P_{shell}=15 Torr; filled symbols are for salt, $C_{feed\text{-}in}$=3 wt%; empty symbols for deionized water)

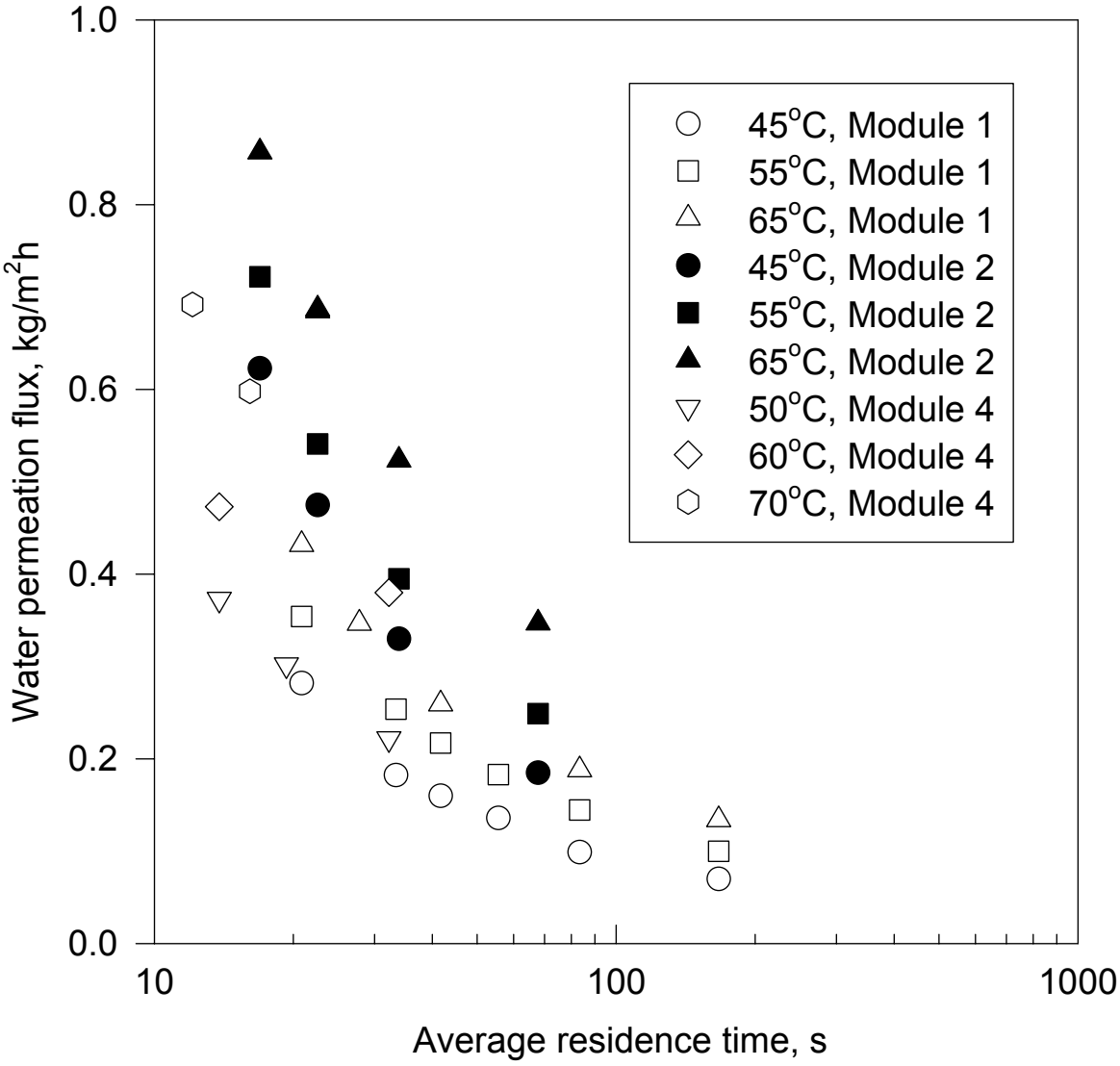

Figure 7. VMD: Effect of silicone coating on the water permeation flux through the membrane when the feed was flowing through the lumen (P_{shell}=15 Torr; deionized water used as feed)

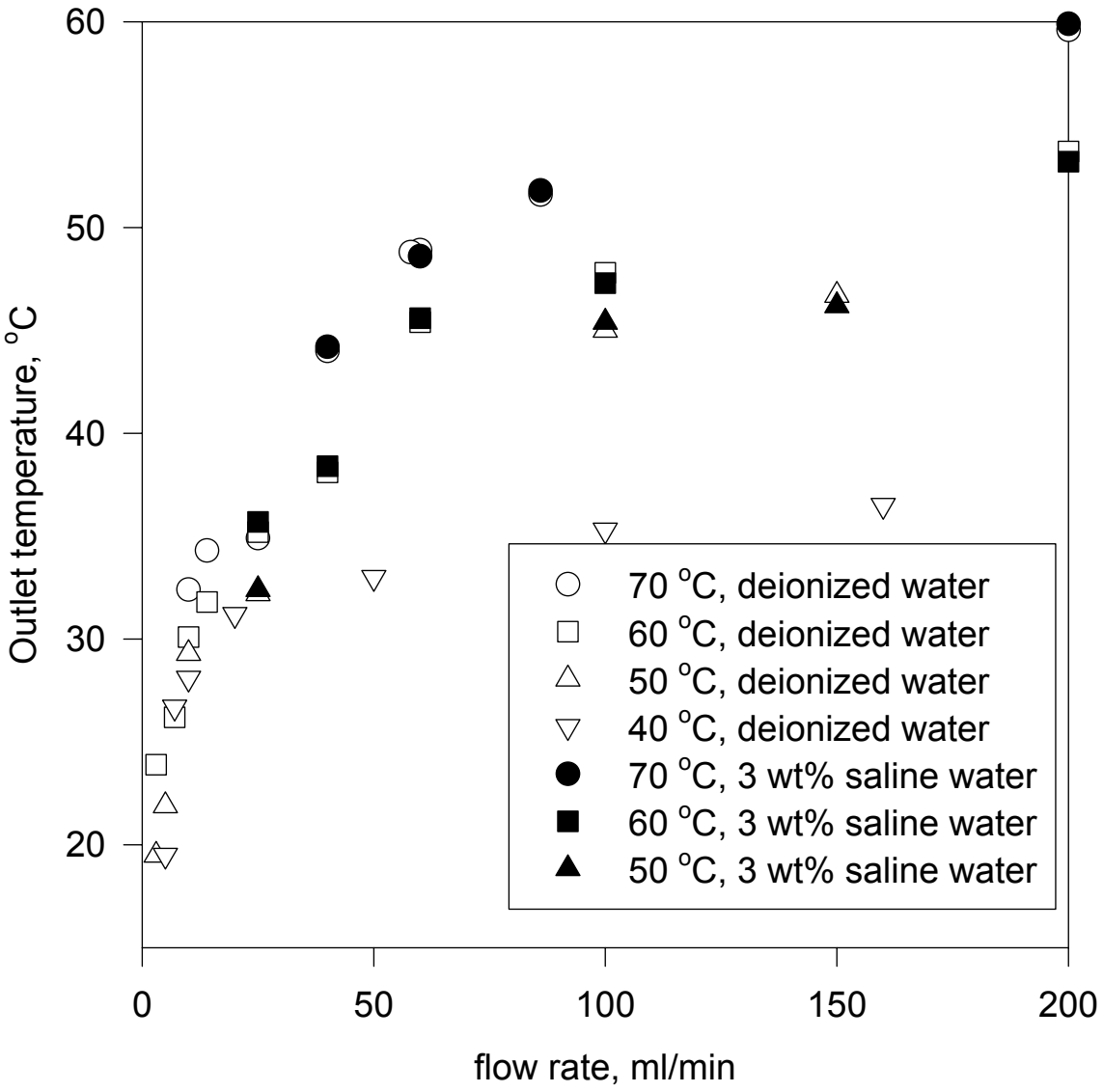

Figure 8. VMD: Variation of feed outlet temperature with feed flow rate through the lumen of hollow fiber module at various feed inlet temperatures (Module 4; P_{shell}=15 Torr)

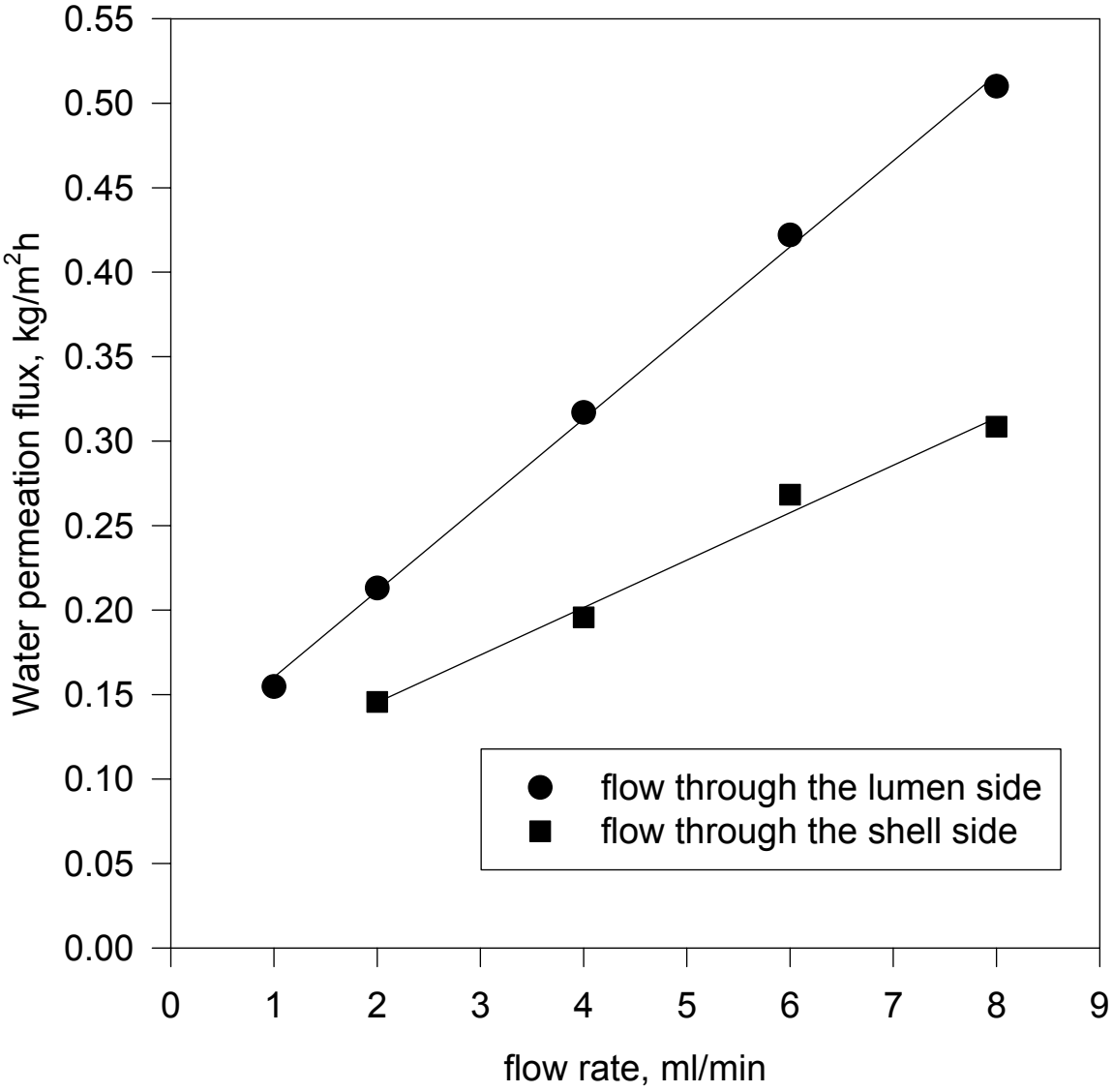

Figure 9. VMD: Variation of water permeation flux with feed-in mode through the hollow fiber module (Module 2; P_{perm}=15 Torr; $T_{feed\text{-}in}$=75^{o}C; deionized water used)

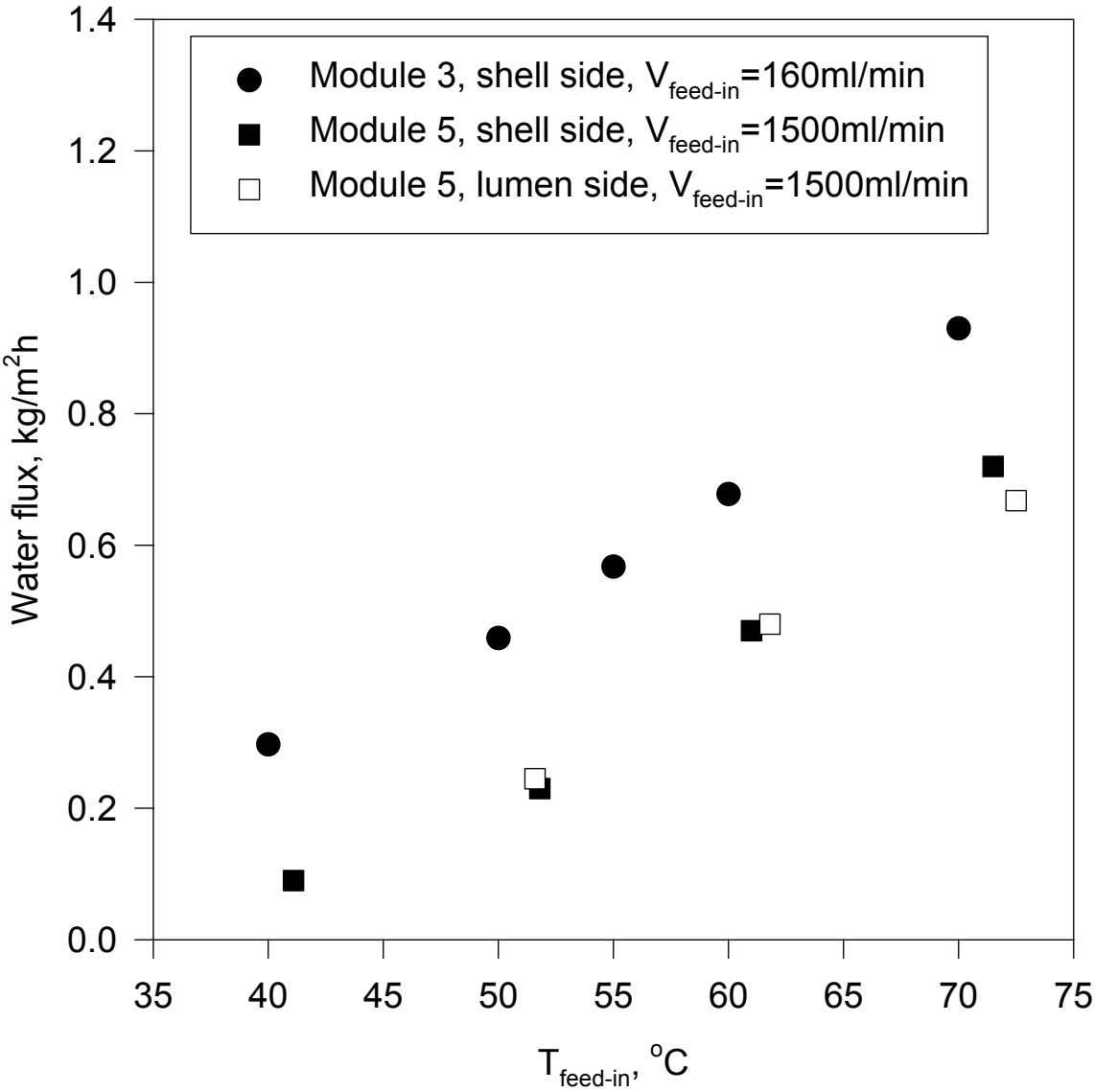

Figure 10. VMD: Variation of water permeation flux with feed inlet temperature (feed was passed through the shell side of cross-flow modules; P_{lumen}=15 Torr; deionized water used as feed)

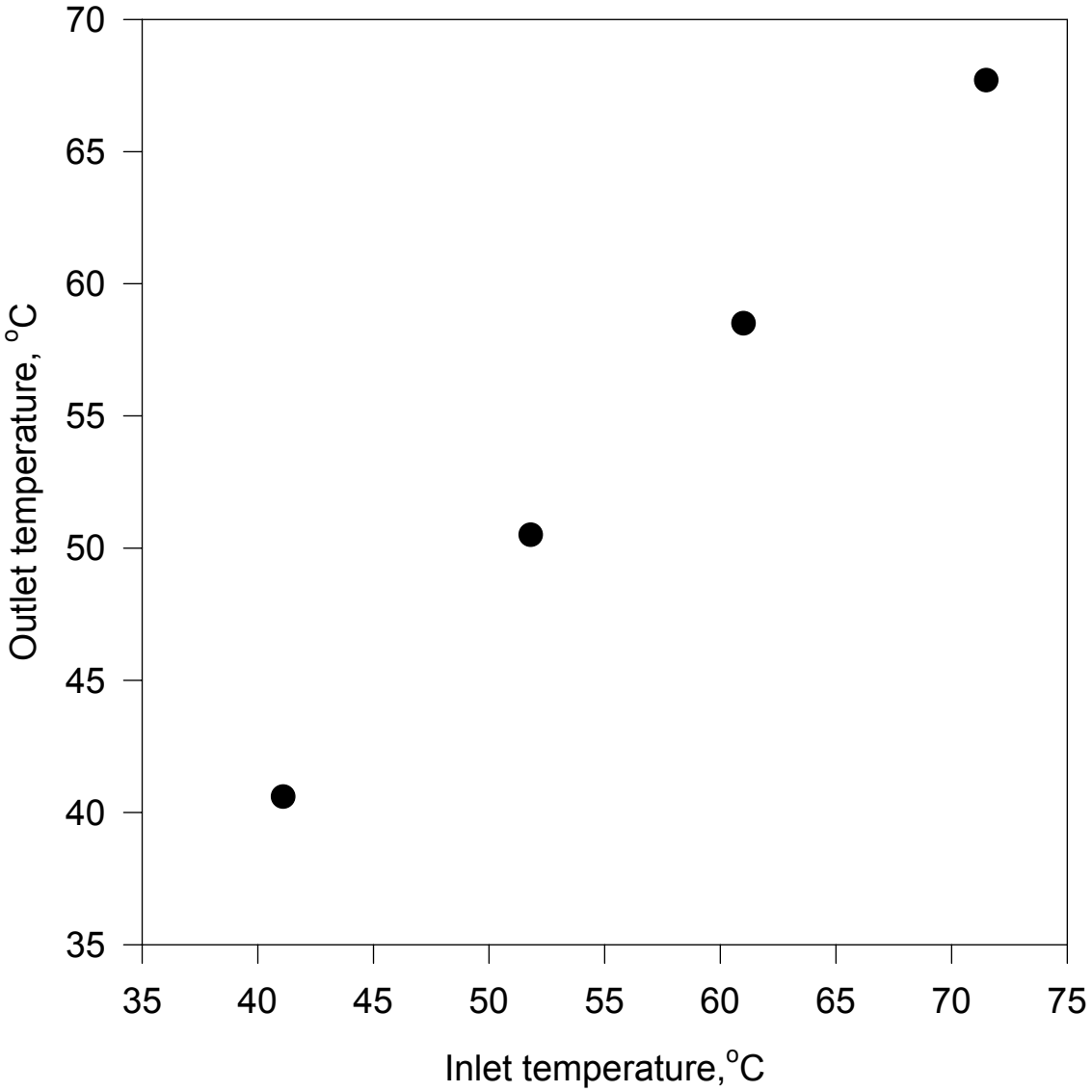

Figure 11. VMD: influence of inlet temperature on the outlet temperature (cross flow Module 5 used, P_{perm}=15 Torr; deionized water used as feed through the shell side; $V_{feed\text{-}in}$=1500 ml/min)

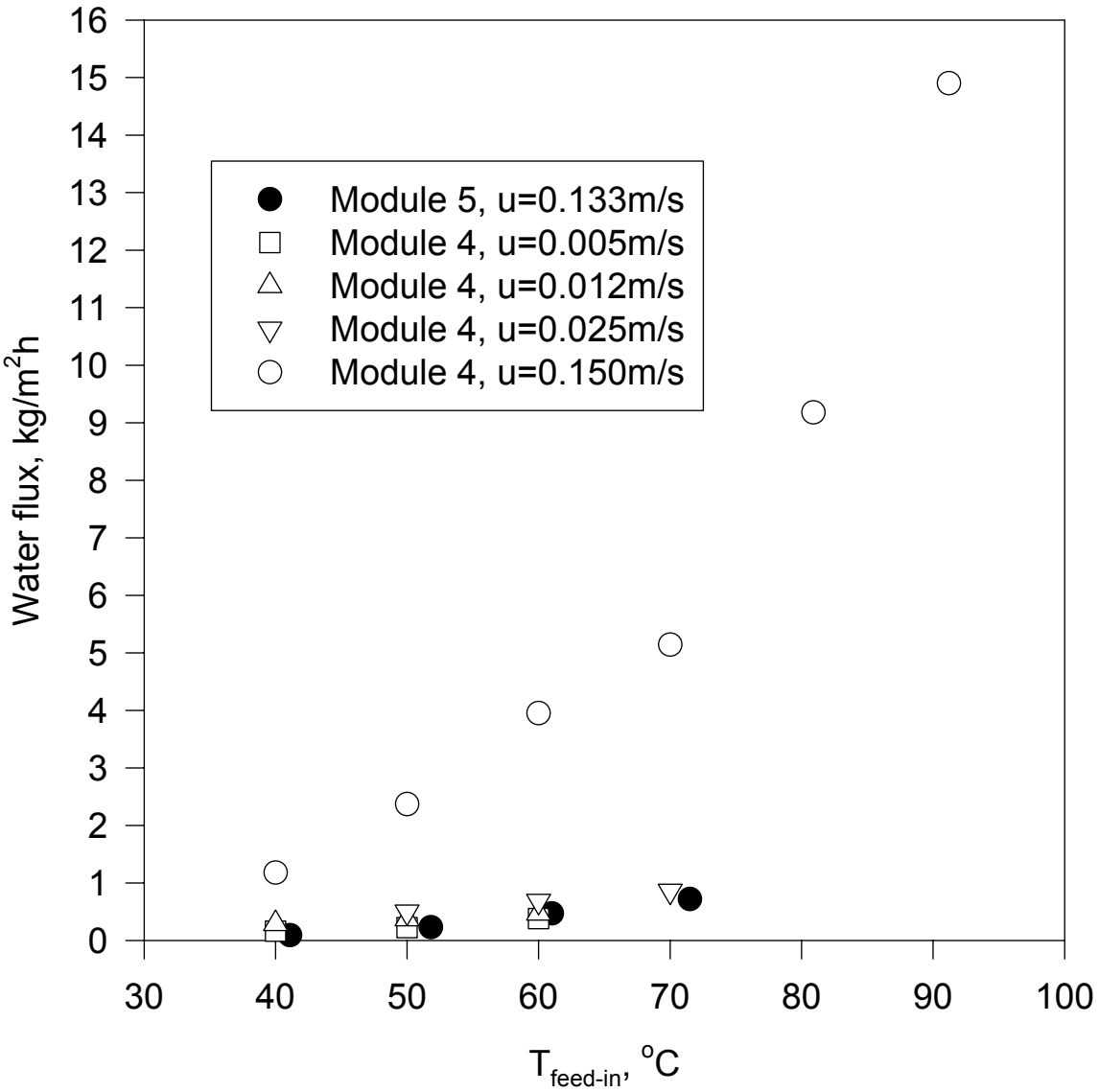

Figure 12. VMD: Influence of different coatings on the water permeation flux (P_{perm}=15 Torr; deionized water used as feed through the lumen)

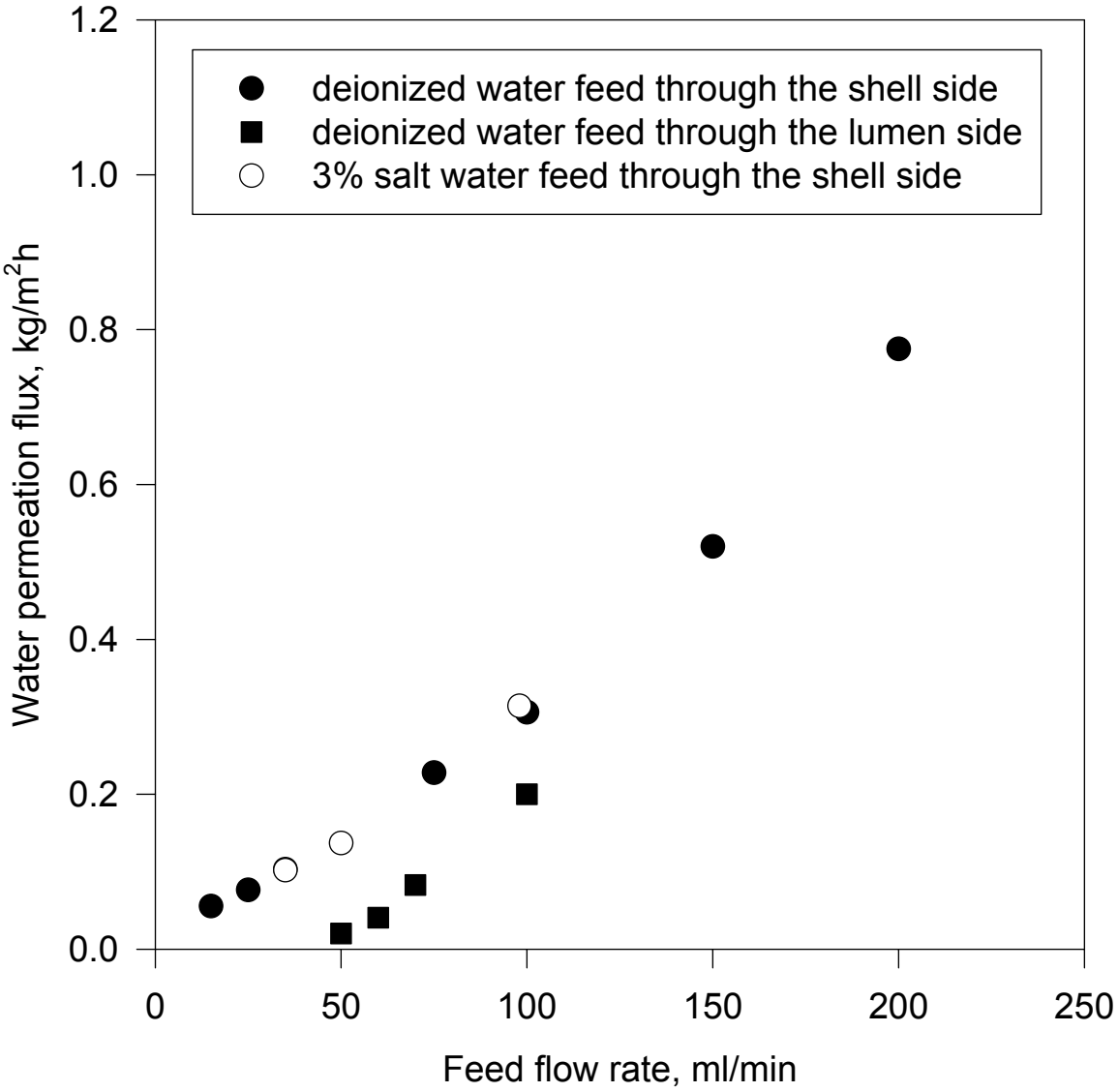

Figure 13. DCMD: water permeation flux at various feed flow rates when the feed and the cooling water were passed countercurrently through the Module 4 ($T_{feed\text{-}in}$=70°C; $T_{cool\text{-}in}$=27.5°C; V_{feed}=V_{cold})

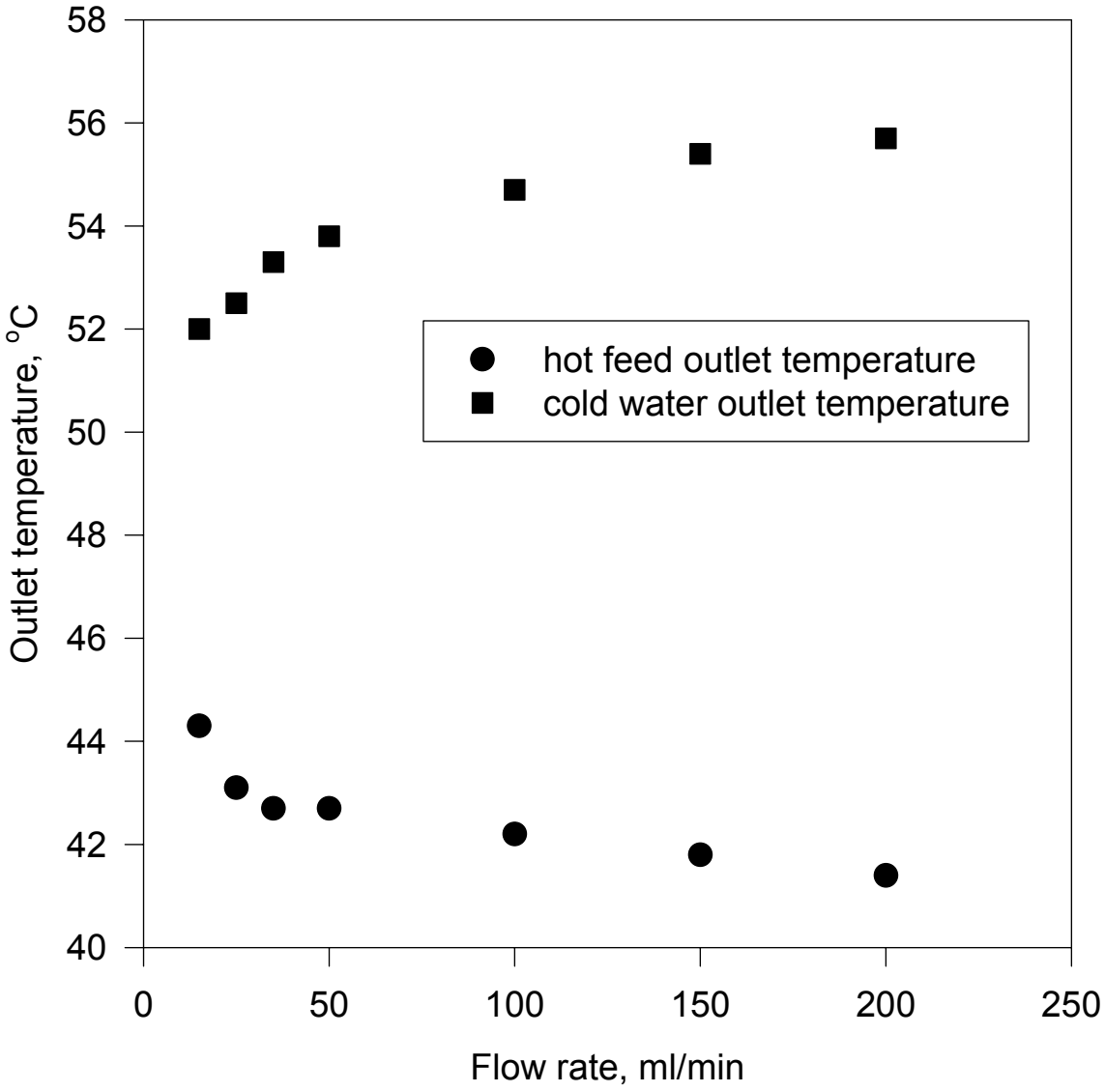

Figure 14. DCMD: outlet temperatures at various flow rates when the hot feed and the cold water were passed countercurrently through the shell and lumen sides of Module 4 respectively (deionized water used, $V_{feed}=V_{cold;}$ $T_{feed\text{-}in}=70^{o}C$; $T_{cold\text{-}in}=27.5^{o}C$)

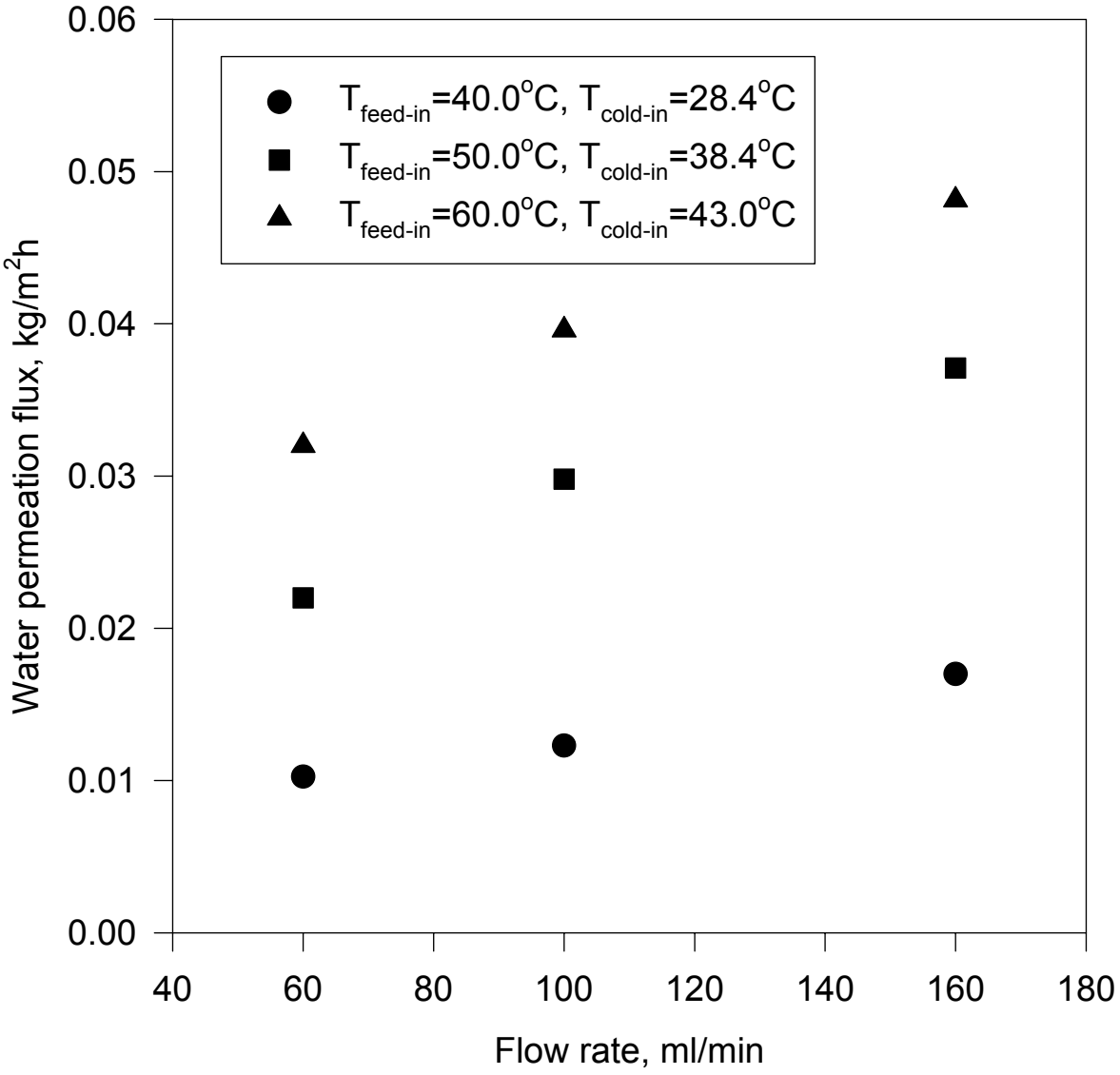

Figure 15. DCMD: variation of water permeation flux with water velocity when 1 wt% saline feed and deionized cooling water were passed through the shell side and lumen side respectively (radial crossflow Module 3 used; V_{feed}=V_{cold}=60 ml/min)

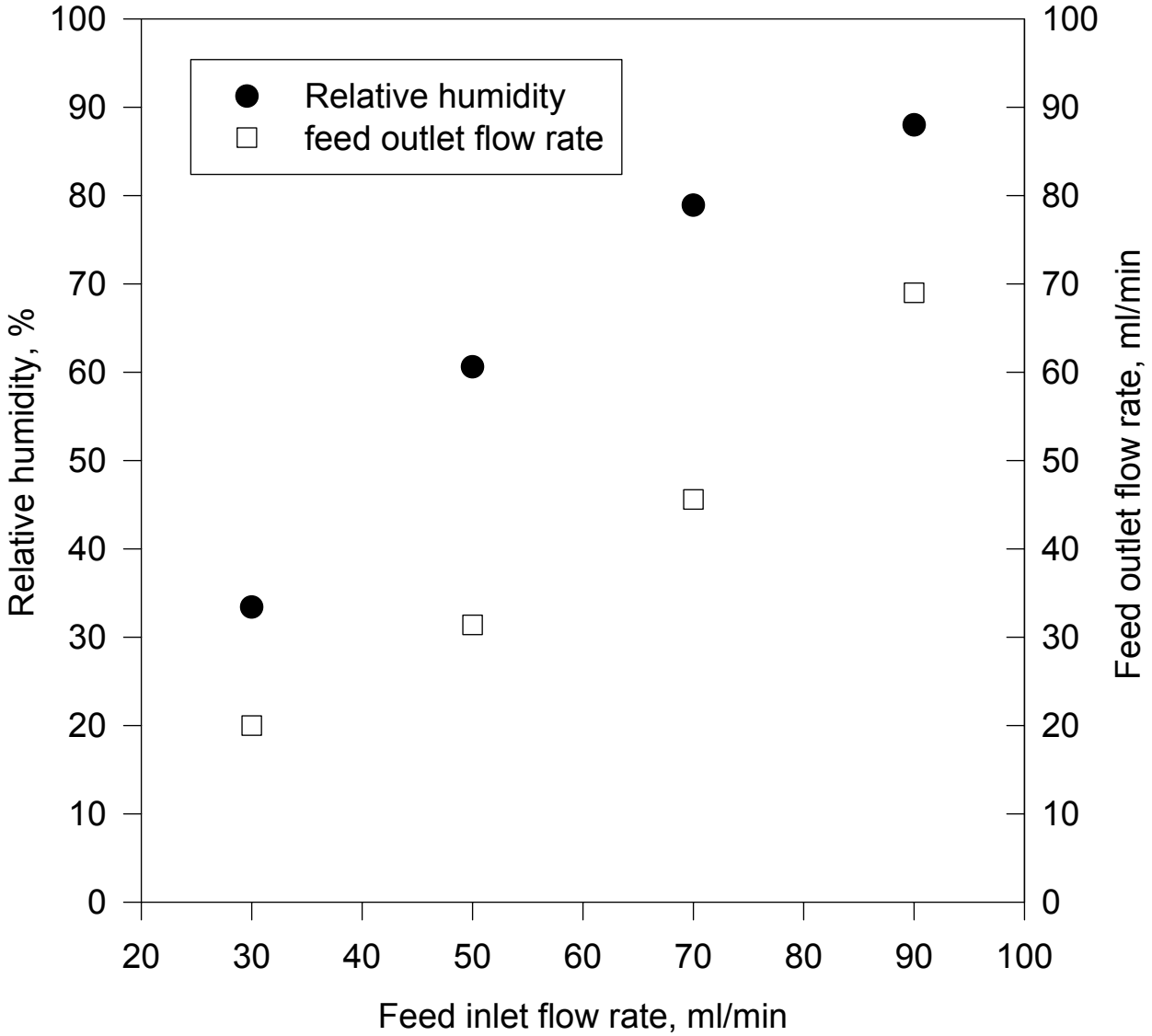

Figure 16. Variation of feed outlet relative humidity and outlet flow rate with feed inlet flow rate (Module 4; the feed was passed co-currently through the lumen; V_{sweep}=150 ml/min; T=22.5 ^{o}C)

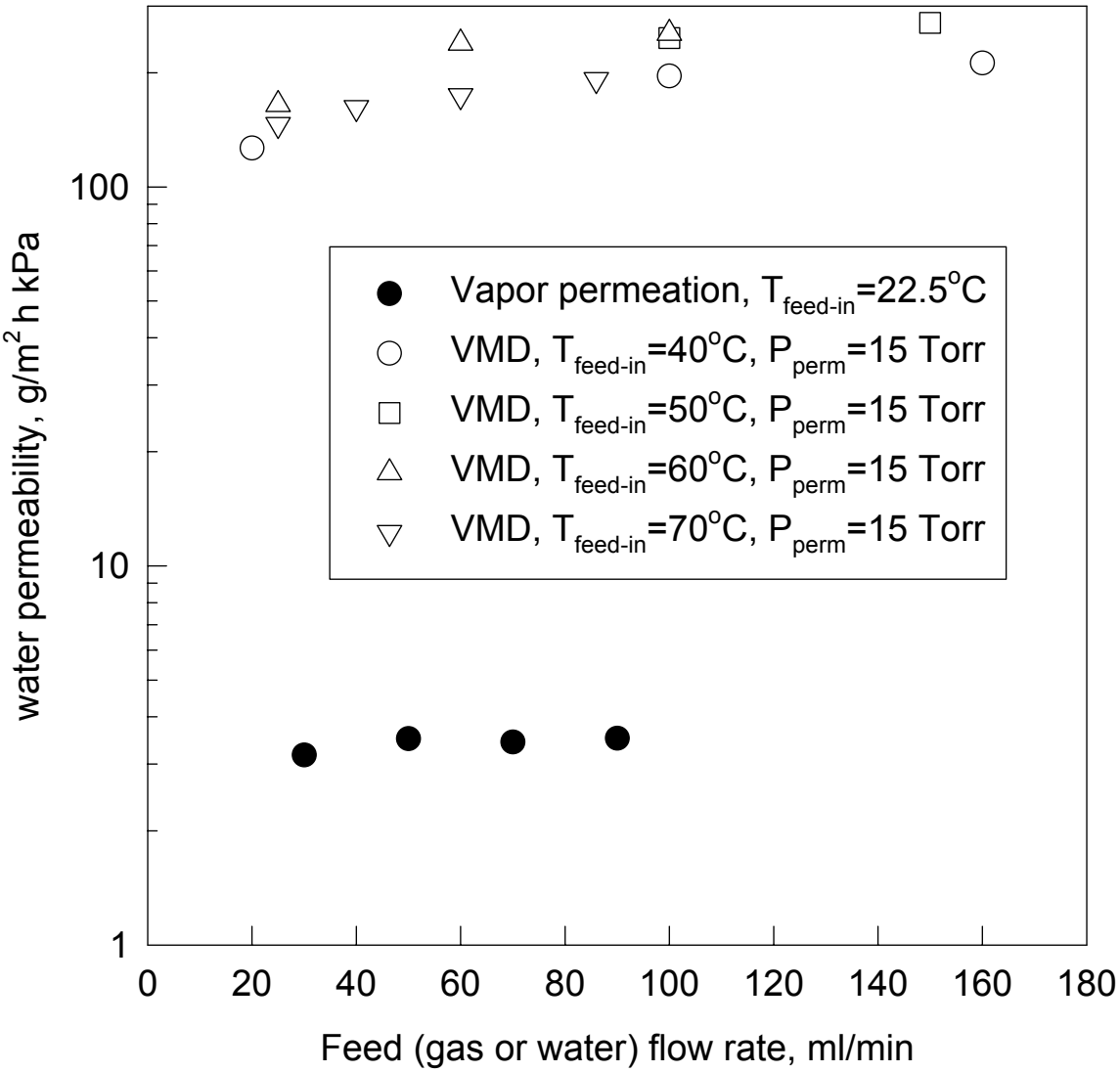

Figure 17. Permeability of water vapor in the vapor permeation tests (Module 4 having silicone coating used; feed gas was passed through the lumen of the module; the sweep gas was passed co-currently through the shell; V_{sweep}=150 ml/min)

Appendix 1

Photograph of setup of Figure 2a

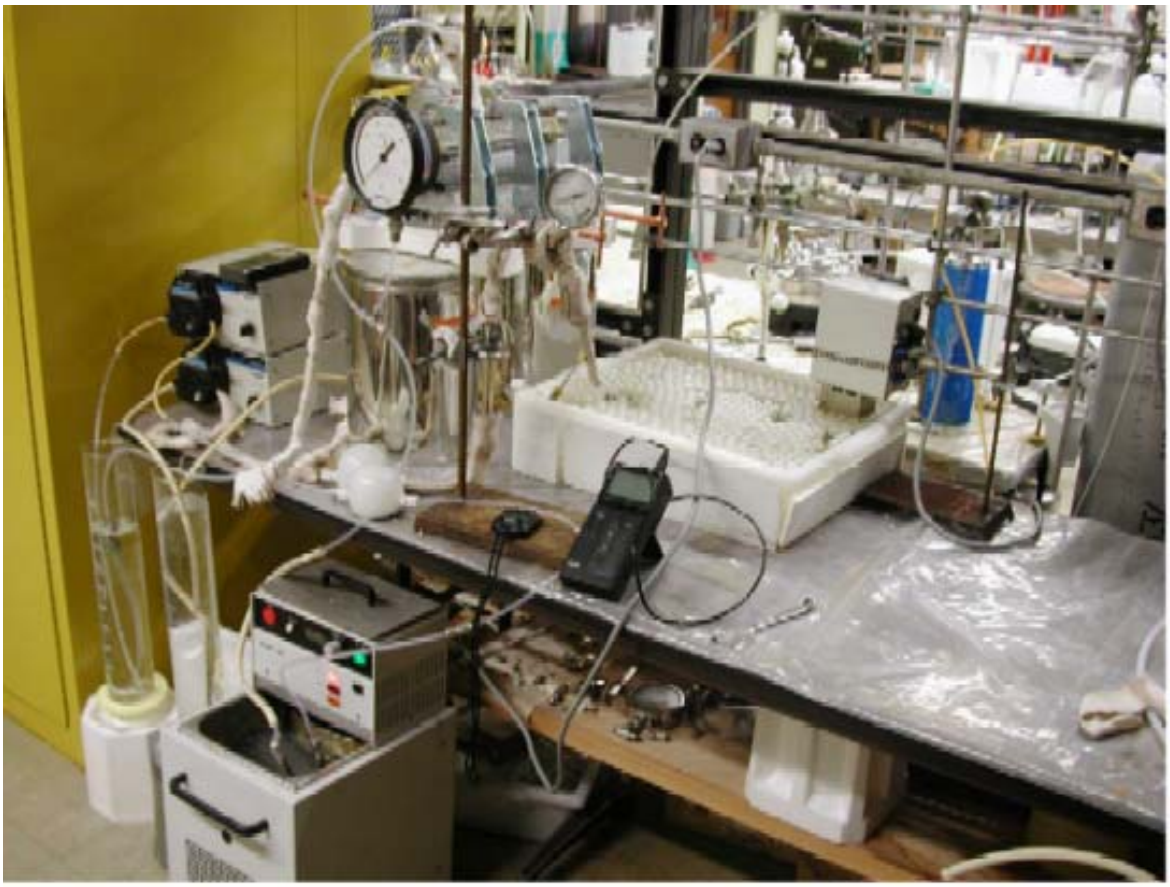

Photograph of Module 4

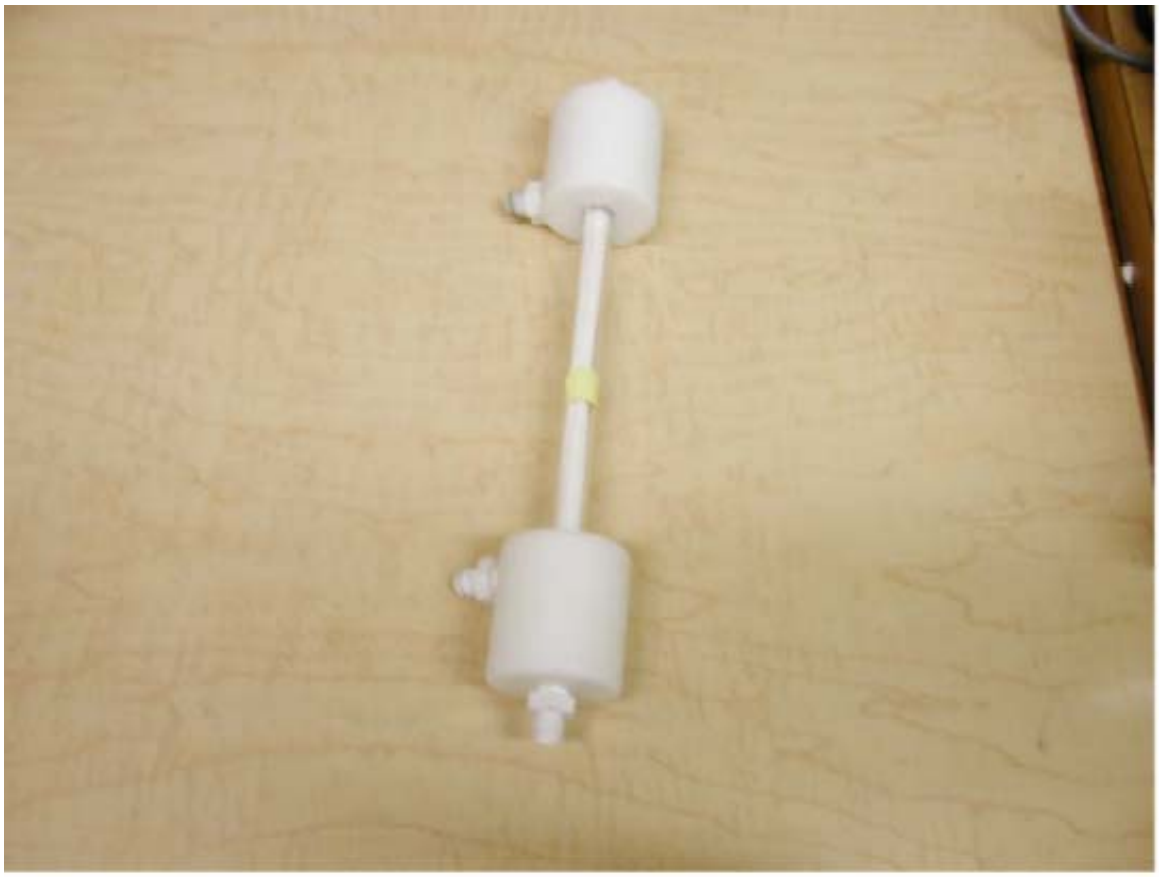

Schematic Figure of Module 3

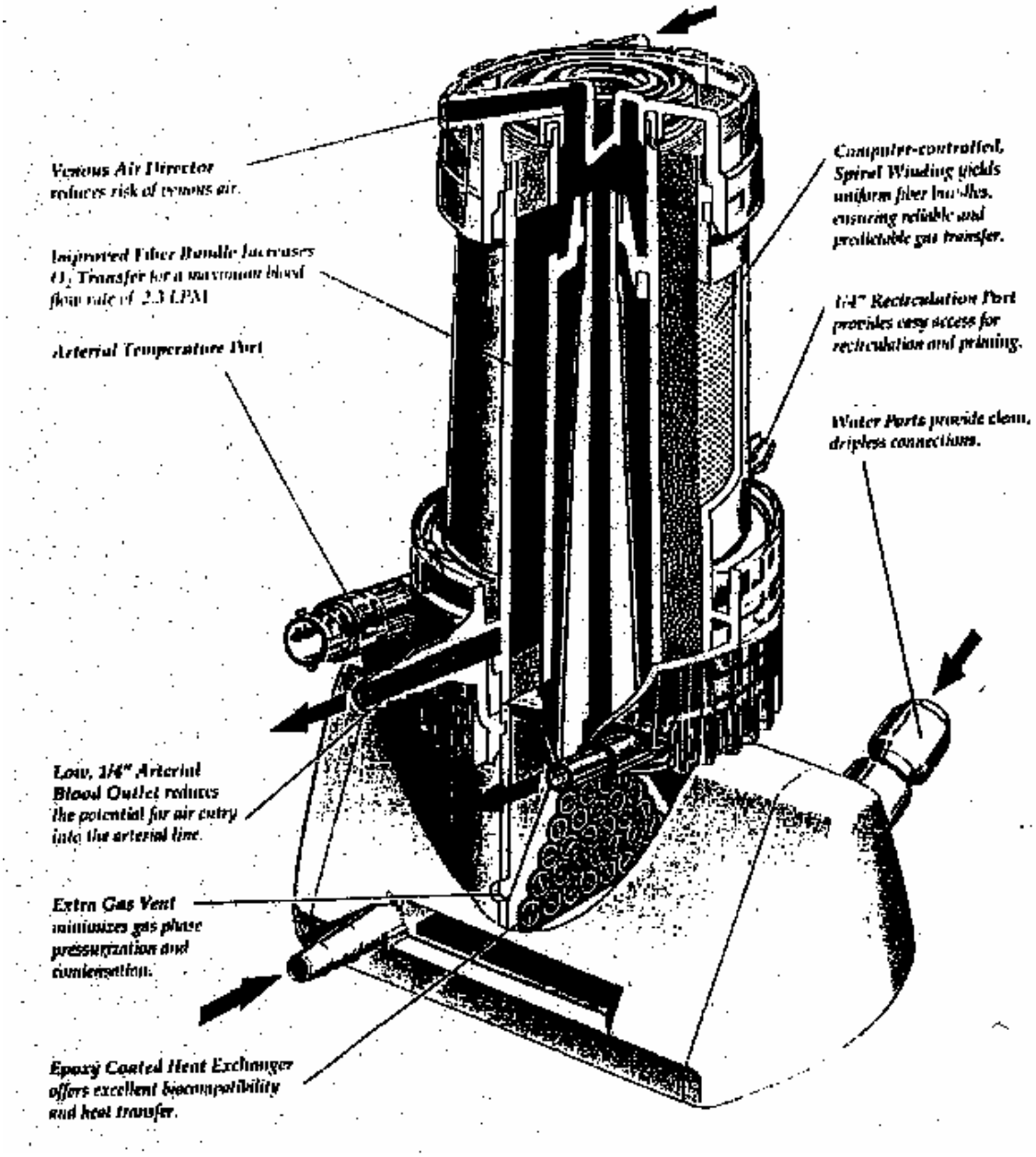

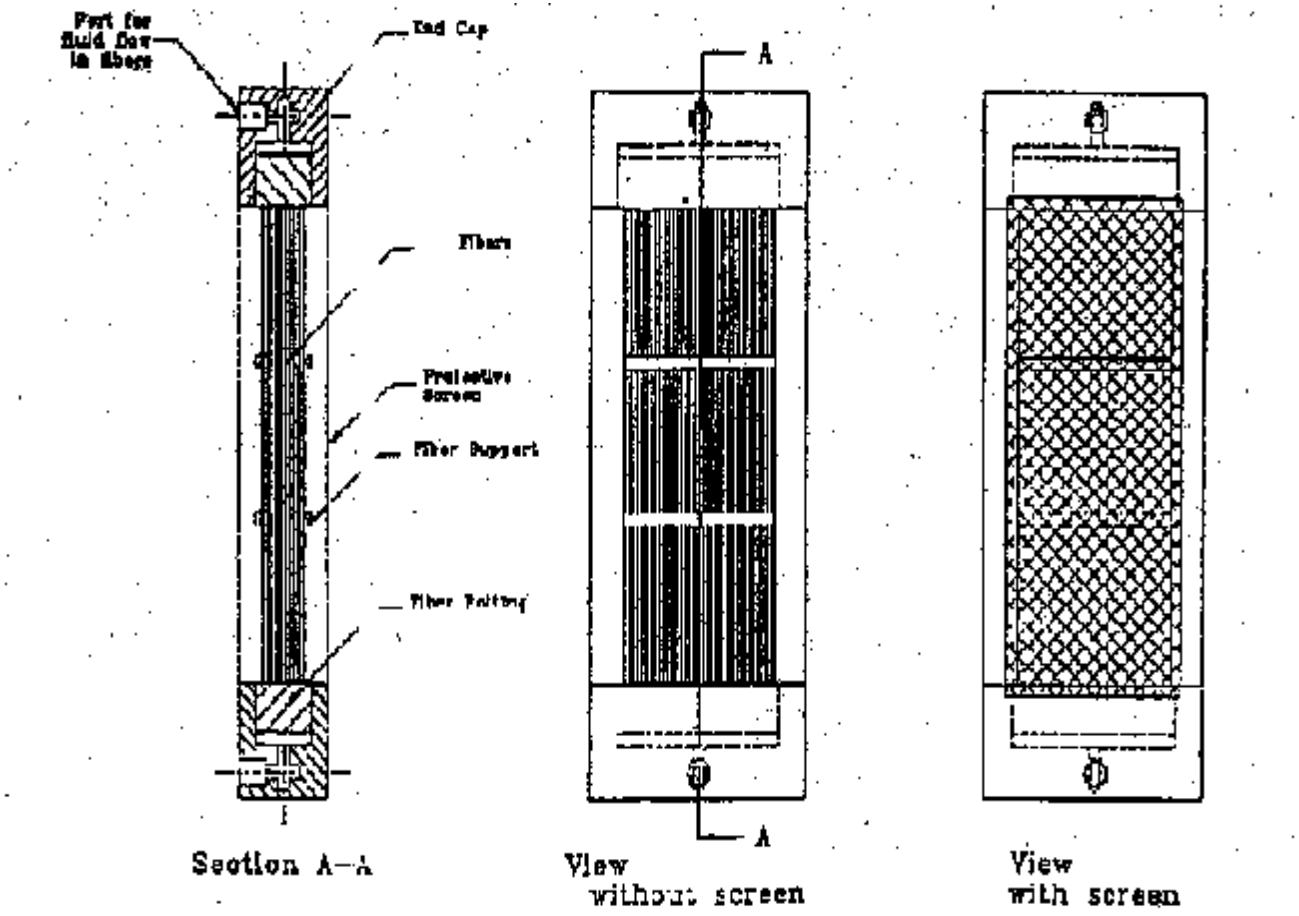

Schematic diagram of Module 5

Appendix 2.

List of Tasks

Task 1:	Procure smaller radial hollow fiber membrane modules
Task 2:	Set up apparatus for DCMD and study performance of smaller modules
Task 3:	Set up a VMD apparatus and study the heat transfer characteristics using smaller modules
Task 4:	Water vapor permeance of the coated fibers
Task 5:	Preliminary DCMD and VMD studies using a larger module
Task 6:	Submit report

Appendix 3

Data Tables

Table A1. VMD experimental data used in Figure 3: variation of water permeation flux with feed water velocity when water was flowing through the lumen of hollow fiber module at various temperatures (Module 2 having porous fibers used; P_{shell}=15 Torr; deionized water used as feed)

Linear velocity, cm/s	Water permeation flux at various feed temperatures, kg/m^{2}h		
	at $T_{feed\text{-}in}$ = 45 ^oC	at $T_{feed\text{-}in}$ = 55 ^oC	at $T_{feed\text{-}in}$ = 65 ^oC
0.47	0.18	0.25	0.34
0.95	0.33	0.39	0.52
1.42	0.48	0.54	0.69
1.89	0.62	0.72	0.86

Table A2. VMD experimental data used in Figure 4: variation of water flux through the membrane with water feed velocity when feed was flowing through the lumen of hollow fibers at various temperatures (Module 1 having silicone coated fibers; deionized water as feed; P_{shell}=15 Torr)

Linear velocity, cm/s	Water permeation flux at various feed temperatures, kg/m^{2}h			
	$T_{feed\text{-}in}$ = 45 ^oC	$T_{feed\text{-}in}$ = 55 ^oC	$T_{feed\text{-}in}$ = 65 ^oC	$T_{feed\text{-}in}$ = 75 ^oC
0.47	0.07	0.10	0.13	0.16
0.94	0.10	0.15	0.19	0.21
1.42	0.14	0.18		
1.89	0.16	0.22	0.26	0.32
2.36	0.18	0.25		
2.83			0.35	0.42
3.78	0.28	0.35	0.43	0.51

Table A3. VMD experimental data used in Figure 5: variation of water permeation flux with water feed velocity when feed was passed through the lumen of hollow fibers at various temperatures (Module 4 having coated fibers; deionized water used as feed; P_{shell}=15 Torr)

velocity, cm/s	Water flux at $T_{feed-in}$ = 40 °C, kg/m^{2}h	velocity, cm/s	Water flux at $T_{feed-in}$ = 50 °C, kg/m^{2}h	velocity, cm/s	Water flux at $T_{feed-in}$ = 60 °C, kg/m^{2}h	velocity, cm/s	Water flux at $T_{feed-in}$ = 70°C, kg/m^{2}h
0.53	0.16	0.53	0.22	0.53	0.38	0.53	0.54
0.88	0.23	0.88	0.30	1.24	0.47	1.06	0.60
1.24	0.29	1.24	0.37	1.77	0.61	1.41	0.69
2.00	0.37	2.50	0.50	2.47	0.68	1.77	0.74
				4.00	0.88	2.47	0.86

Table A4. VMD experimental data used in Figure 6: variation of water flux with water feed velocity when feed was passed through the lumen of hollow fibers at various temperatures (Module 4; P_{shell}=15 Torr)

deionized water used as feed								brine feed, $C_{feed-in}$=3 wt%			
u*, cm/s	F** at T=40°C, kg/m^{2}h	u, cm/s	F at T=50°C, kg/m^{2}h	u, cm/s	F at T=60°C, kg/m^{2}h	u, cm/s	F at T=70°C, kg/m^{2}h	u, cm/s	F at T=50°C, kg/m^{2}h	u, cm/s	F at T=50°C, kg/m^{2}h
0.53	0.25	0.53	0.22	0.53	0.58	1.06	0.66	0.55	0.34	1.00	0.66
0.88	0.34	0.88	0.30	1.24	0.72	1.41	0.77	0.84	0.48	1.44	0.77
1.24	0.44	1.24	0.37	1.77	0.92	1.77	0.98	1.21	0.56	1.90	0.94
4.04	0.78	4.42	1.51	2.47	1.04	2.47	1.19	4.65	1.51	2.40	1.21
5.60	0.87	7.70	1.84	4.42	2.12	4.30	2.70	7.70	1.86	4.34	2.65
11.2	1.09	17.7	2.37	10.8	3.56	6.70	2.99	16.1	2.30	6.87	3.26
17.7	1.28	31.8	2.79	17.8	3.95	9.00	3.70	30.0	2.67	15.3	5.10
27.8	1.43			35.4	5.14	15.2	5.15			35.6	6.49
						35.4	6.61				

* linear velocity of feed passing through the lumen of fibers, cm/s

** water permeation flux through the membrane, kg/m^{2}h

Table A5. VMD experimental data used in Figure 7: effect of silicone coating on the water permeation flux through the membrane when the feed was flowing through the lumen (P_{shell}=15 Torr; deionized water used as feed)

Module 1				Module 2				Module 4					
τ*, s	F** at 45°C	F at 55°C	F at 65°C	τ, s	F at 45°C	F at 55°C	F at 65°C	τ, s	F at 50°C	τ, s	F at 60°C	τ, s	F at 70°C
167	0.07	0.10	0.13	67.7	0.19	0.25	0.35	32.2	0.22	32.2	0.38	16.1	0.60
83.4	0.10	0.15	0.19	33.9	0.33	0.40	0.53	19.3	0.30	13.8	0.47	12.1	0.69
55.6	0.14	0.18		22.6	0.48	0.54	0.69	13.8	0.37	9.55	0.61	9.66	0.74
41.7	0.16	0.22	0.26	16.9	0.62	0.72	0.86	6.84	0.50	6.91	0.68	6.91	0.86
33.3	0.18	0.25								4.28	0.88		
27.8			0.35										
20.6	0.28	0.35	0.43										

* Average residence time of feed passing through the lumen of fibers, s
** water permeation flux through the membrane, kg/m^{2}h

Table A6. VMD experimental data used in Figure 8: variation of feed outlet temperature with feed flow rate through the lumen of hollow fiber module at various feed inlet temperatures (Module 4; P_{shell}=15 Torr)

$T_{feed-out}$ (°C) when $T_{feed-in}$=70 °C			$T_{feed-out}$ (°C) when $T_{feed-in}$ =60 °C			$T_{feed-out}$ (°C) when $T_{feed-in}$ =50 °C			$T_{feed-out}$ (°C) when $T_{feed-in}$ =40 °C	
V, ml/min	water	brine, 3 wt%	V, ml/min	water	brine, 3 wt%	V, ml/min	water	brine, 3 wt%	V, ml/min	water
10.0	32.4		3.0	23.9		3.0	19.5		5.0	19.5
14.0	34.3		7.0	26.2		5.0	21.9		7.0	26.7
25.0	34.9		10.0	30.1		10.0	29.3		10.0	28.1
40.0	44.0	44.2	14.0	31.8		25.0	32.2	32.4	20.0	31.2
58.0	48.8		25.0	35.2	35.7	100	45.0	45.4	50.0	33.0
60.0	48.9	48.6	40.0	38.1	38.4	150	46.7	46.2	100.0	35.3
86.0	51.6	51.9	60.0	45.4	45.6				160.0	36.5
200	59.6	59.9	100	47.8	47.3					
			200	53.7	53.2					

V Flow rate of feed passing through the lumen of fibers, ml/min
$T_{feed-out}$ Temperature of feed at outlet, °C

Table A7. VMD experimental data used in Figure 9: Variation of water permeation flux with feed-in mode through the hollow fiber module (Module 2; P_{perm}=15 Torr; $T_{feed\text{-}in}$= 75^{o}C; deionized water used)

	Water permeation flux, kg/m^{2}h	
Flow rate, ml/min	When feed was flowing through the lumen side	When feed was flowing through the shell side
1.0	0.15	
2.0	0.21	0.15
4.0	0.32	0.20
6.0	0.42	0.27
8.0	0.51	0.31

Table A8. VMD experimental data used in Figure 10: variation of water permeation flux with feed inlet temperature (feed was passed through the shell side of cross-flow modules; P_{lumen}=15 Torr; deionized water used as feed)

Module 3, shell side$V_{feed\text{-}in}$ =160 ml/min		Module 5, shell side$V_{feed\text{-}in}$ =1500 ml/min		Module 5, shell side$V_{feed\text{-}in}$ =1500 ml/min	
$T_{feed\text{-}in}$, ^{o}C	Water permeation flux, kg/m^{2}h	$T_{feed\text{-}in}$, ^{o}C	Water permeation flux, kg/m^{2}h	$T_{feed\text{-}in}$, ^{o}C	Water permeation flux, kg/m^{2}h
40.0	0.297	41.1	0.09	51.6	0.245
50.0	0.459	51.8	0.23	61.8	0.480
55.0	0.567	61.0	0.47	72.5	0.668
60.0	0.678	71.5	0.72		
70.0	0.930				

Table A9. VMD experimental data used in Figure 11: influence of inlet temperature on the outlet temperature (cross flow Module 5 used, P_{perm}=15 Torr; deionized water used as feed through the shell side; $V_{feed\text{-}in}$=1500ml/min)

$T_{feed\text{-}in}$, ^{o}C	$T_{feed\text{-}out}$, ^{o}C
41.1	40.6
51.8	50.5
61.0	58.5
71.5	67.7

Table A10. Experimental data used in Figure 12. VMD: Influence of different coatings on the water permeation flux (P_{perm}=15 Torr*; deionized water used as feed passed through the lumen)

Module 5		Module 4							
u**=0.133 m/s		u**=0.005 m/s		u**=0.012 m/s		u**=0.025 m/s		u**=0.150m/s	
$T_{feed\text{-}in}$, ^{o}C	Water flux, kg/m^2h	$T_{feed\text{-}in}$, ^{o}C	Water flux, kg/m^2h	$T_{feed\text{-}in}$, ^{o}C	Water flux, kg/m^2h	$T_{feed\text{-}in}$, ^{o}C	Water flux, kg/m^2h	$T_{feed\text{-}in}$, ^{o}C	Water flux, kg/m^2h
41.1	0.09	40.0	0.163	40.0	0.290	40.0		40.0	1.18
51.8	0.23	50.0	0.222	50.0	0.373	50.0	0.497	50.0	2.37
61.0	0.47	60.0	0.380	60.0	0.473	60.0	0.683	60.0	3.95
71.5	0.72	70.0		70.0		70.0	0.860	70.0	5.14
								80.9	9.18
								91.2	14.9

* 15 Torr is at the vacuum pump inlet; the pressure at the shell is much higher. For example at, 80.9 and 91.2 ^{o}C, the shell side pressure might be higher than 130 Torr.

** linear velocity of feed flowing through the lumen of the fibers, m/s

Table A11. DCMD experimental data used in Figure 13: water permeation flux at various feed flow rates when the feed and the cooling water were passed countercurrently through the Module 4 (V_{feed}=$V_{cold;}$ $T_{feed\text{-}in}$ =70 ^{o}C; $T_{cool\text{-}in}$ =27.5 ^{o}C)

Deionized water feed flowing through the shell side		3 wt% brine feed flowing through the shell side		Deionized water feed flowing through the lumen side	
Flow rate, ml/min	Water permeation flux, kg/m^{2}h	Flow rate, ml/min	Water permeation flux, kg/m^{2}h	Flow rate, ml/min	Water permeation flux, kg/m^{2}h
15.0	0.056			50.0	0.02
25.0	0.076			60.0	0.04
35.0	0.103	35.0	0.102	70.0	0.08
50.0		50.0	0.137	100.0	0.20
75.0	0.228				
100.0	0.306	98.0	0.314		
150.0	0.520				
200.0	0.775				

Table A12. DCMD experimental data used in Figure 14: outlet temperatures at various flow rates when the hot feed and the cold water were passed countercurrently through the shell and lumen sides of Module 4 respectively (V_{feed}=V_{cold}; $T_{feed\text{-}in}$=70^{o}C; $T_{cold\text{-}in}$=27.5^{o}C)

Feed flow rate, ml/min	Feed outlet temperature, ^{o}C	Cooling water outlet temperature, ^{o}C
15	44.3	52.0
25	43.1	52.5
35	42.7	53.3
50	42.7	53.8
100	42.2	54.7
150	41.8	55.4
200	41.4	55.7

Table A13. DCMD experimental data used in Figure 15: variation of water permeation flux through the membrane with water velocity when feed and cooling water were passed through the shell side and lumen side respectively (cross-flow Module 3 used; 1 wt% brine feed V_{feed}=60 ml/min, deionized cooling water V_{cold}=60 ml/min)

	Water permeation flux, kg/m^{2}h		
Feed flow rate, ml/min	When $T_{feed\text{-}in}$=40 ^oC, and $T_{cold\text{-}in}$=28.4 ^oC	When $T_{feed\text{-}in}$=50 ^oC, and $T_{cold\text{-}in}$=38.4 ^oC	When $T_{feed\text{-}in}$=60 ^oC, and $T_{cold\text{-}in}$=43.0 ^oC
60.0	0.010	0.022	0.032
100.0	0.012	0.030	0.040
160.0	0.017	0.037	0.048

Table A14. Experimental data used in Figure 16. Variation of feed outlet relative humidity and outlet flow rate with feed inlet flow rate (Module 4; the feed N_2 was passed co-currently through the lumen flow; V_{sweep}=150 ml/min; T=22.5 ^oC)

Feed flow rate, ml/min	Relative humidity, %	Feed outlet flow rate, ml/min
30.0	33.4	20.0
50.0	60.6	31.4
70.0	78.9	45.6
90.0	88.0	69.0

Table A15. Experimental data used in Figure 17. Permeability of water vapor in the vapor permeation tests (Module 4 having silicone coating used; feed gas was passed through the lumen of the module; the sweep gas was passed co-currently through the shell in the vapor permeation; V_{sweep}=150 ml/min. In the VMD, the feed water was passed through the lumen side; P_{shell}=15 Torr)

Vapor permeation,		Vacuum membrane distillation							
$T_{feed-in}$=22.5^{o}C		$T_{feed-in}$=40.0 ^{o}C		$T_{feed-in}$=50.0 ^{o}C		$T_{feed-in}$=60.0 ^{o}C		$T_{feed-in}$=70.0 ^{o}C	
Flow rate, ml/min	Water permea., g/m^{2}h kPa	Flow rate, ml/min	Water permea., g/m^{2}h kPa	Flow rate, ml/min	Water permea., g/m^{2}h kPa	Flow rate, ml/min	Water permea., g/m^{2}h kPa	Flow rate, ml/min	Water permea., g/m^{2}h kPa
30.0 50.0 70.0 90.0	33.4 60.6 78.9 86.8	20.0 100.0 160.0	127 196 212	25.0 100.0 150.0	314 247 271	25.0 60.0 100.0	165 239 254	25.0 40.0 86.0 60.0	146 162 192 174